Basic Research in Cardiology (2023) 118:3
https://doi.org/10.1007/s00395-022-00976-x

ORIGINAL CONTRIBUTION

Reduction in mitochondrial ROS improves oxidative phosphorylation and provides resilience to coronary endothelium in non-reperfused myocardial infarction

Rayane Brinck Teixeira[1] · Melissa Pfeiffer[1] · Peng Zhang[2] · Ehtesham Shafique[1] · Bonnie Rayta[1] · Catherine Karbasiafshar[1] · Nagib Ahsan[3,4,5] · Frank W. Sellke[1] · M. Ruhul Abid[1]

Received: 9 March 2022 / Revised: 30 December 2022 / Accepted: 30 December 2022 / Published online: 13 January 2023

Abstract

Recent studies demonstrated that mitochondrial antioxidant MnSOD that reduces mitochondrial (mito) reactive oxygen species (ROS) helps maintain an optimal balance between sub-cellular ROS levels in coronary vascular endothelial cells (ECs). However, it is not known whether EC-specific mito-ROS modulation provides resilience to coronary ECs after a non-reperfused acute myocardial infarction (MI). This study examined whether a reduction in endothelium-specific mito-ROS improves the survival and proliferation of coronary ECs in vivo. We generated a novel conditional binary transgenic animal model that overexpresses (OE) mitochondrial antioxidant MnSOD in an EC-specific manner (MnSOD-OE). EC-specific MnSOD-OE was validated in heart sections and mouse heart ECs (MHECs). Mitosox and mito-roGFP assays demonstrated that MnSOD-OE resulted in a 50% reduction in mito-ROS in MHEC. Control and MnSOD-OE mice were subject to non-reperfusion MI surgery, echocardiography, and heart harvest. In post-MI hearts, MnSOD-OE promoted EC proliferation (by 2.4 ± 0.9 fold) and coronary angiogenesis (by 3.4 ± 0.9 fold), reduced myocardial infarct size (by 27%), and improved left ventricle ejection fraction (by 16%) and fractional shortening (by 20%). Interestingly, proteomic and Western blot analyses demonstrated upregulation in mitochondrial complex I and oxidative phosphorylation (OXPHOS) proteins in MnSOD-OE MHECs. These MHECs also showed increased mitochondrial oxygen consumption rate (OCR) and membrane potential. These findings suggest that mito-ROS reduction in EC improves coronary angiogenesis and cardiac function in non-reperfused MI, which are associated with increased activation of OXPHOS in EC-mitochondria. Activation of an energy-efficient mechanism in EC may be a novel mechanism to confer resilience to coronary EC during MI.

Keywords Myocardial infarction · Angiogenesis · MnSOD · Endothelial cell · Oxidative stress · OXPHOS

Abbreviations

ROS	Reactive oxygen species
MI	Myocardial infarction
MnSOD	Manganese superoxide dismutase, superoxide dismutase 2, mitochondrial specific isoform of superoxide dismutase enzyme

✉ M. Ruhul Abid
ruhul_abid@brown.edu

1 Division of Cardiothoracic Surgery, Department of Surgery, Cardiovascular Research Center, Rhode Island Hospital, Brown University Warren Alpert Medical School, 1 Hoppin Street, Providence, RI 02903, USA

2 Vascular Research Laboratory/Providence VA Medical Center and Department of Medicine, Alpert Medical School of Brown University, Providence, RI, USA

3 Division of Biology and Medicine, Alpert Medical School, Brown University, Providence, RI 02903, USA

4 Proteomics Core Facility, Center for Cancer Research and Development, Rhode Island Hospital, Providence, RI 02903, USA

5 Present Address: Department of Chemistry and Biochemistry, Mass Spectrometry, Proteomics and Metabolomics Core Facility, Stephenson Life Sciences Research Center, University of Oklahoma, Norman, OK, USA

EC	Endothelial cell
MnSOD Tet-ON/Tet-OFF	Double transgenic model that presents normal (Tet-ON) or overexpression (Tet-OFF) of MnSOD specifically in endothelial cells
OE	Overexpression
LAD	Left anterior descending coronary artery
MHEC	Mouse heart endothelial cell
ERK	Extracellular signal-regulated kinase, also known as mitogen-activated protein kinase (MAPK)
CVD	Cardiovascular disease
NO	Nitric oxide
NOX2	NADPH oxidase 2
AMPK	AMP kinase
eNOS	Endothelial isoform of nitric oxide synthase
mito-ROS	Mitochondrial reactive oxygen species
tTA	Tetracycline-controlled transactivator
VE-cad	Vascular endothelial cadherin
PCR	Polymerase chain reaction
Mito-roGFP	Mitochondria-targeted adenovirus construct
BME	Basement membrane extract
EF	Ejection fraction
FS	Fractional shortening
FAC	Fractional area change
ESV	End systolic volume
EDV	End diastolic volume
SAWT	Systolic anterior wall thickness
DAWT	Diastolic anterior wall thickness
SPWT	Systolic posterior wall thickness
DPWT	Diastolic posterior wall thickness
PCNA	Proliferating cell nuclear antigen
αSMA	α-Smooth muscle actin
LV	Left ventricular
ETS	Erythroblast transformation-specific
VEGF	Vascular endothelial growth factor
ERG	Erythroblast transformation-specific related gene
OXPHOS	Oxidative phosphorylation

Introduction

Cardiovascular disease (CVD) has been the leading cause of death in the world for the last few decades, with the current prevalence at 48% in the adult population of the United States [10, 63]. Ischemic heart disease alone is the major contributor to CVD deaths and consists of a series of events involved in endothelial dysfunction that ultimately leads to acute myocardial infarction (MI) and eventual heart failure. The widespread prevalence and mortality rates of CVD necessitate further study into cardiovascular pathophysiology and potential therapeutics.

Endothelial cells (ECs) are the most abundant cell type in the adult heart and vasculature. Lining the inner layer of blood vessels, ECs are essential for the homeostasis of blood supply and cardioprotection [24, 25]. Although presenting high plasticity, ECs undertake considerable stress in the occurrence of MI and reperfusion therapy, resulting in loss of EC permeability, barrier function, inflammatory homeostasis, and microvascular obstruction [24, 26, 41, 58]. Numerous ECs are lost via several cell death processes after MI affecting coronary vascular density in ischemic regions, which in turn further deteriorates recovery of post-MI cardiac function [65]. To address this loss of coronary ECs, increasing EC resilience and/or induction of angiogenesis, i.e. sprouting of new blood vessels, have been a target of recent studies with the goal of restoring microcirculation to limit or prevent post-MI cardiac remodeling [34, 60]. Reactive oxygen species (ROS) have been shown to be of special pathophysiological importance in EC survival and proliferation in health and disease as well as in CVD including ischemic myocardium [20, 40, 44]. Early pre-clinical research with antioxidant supplements, such as ascorbic acid and retinoic acid, showed promising benefits and post-MI protection of cardiovascular function [43, 61]. However, most recent clinical trials showed controversial results or even increased overall mortality with various antioxidant treatments that target total cellular/global ROS levels, suggesting a critical role for subcellular ROS rather than global ROS [11, 12].

In EC, intracellular ROS are generated from several different sources including NADPH oxidases, mitochondria, cytochrome P450 and xanthine oxidase [3, 23, 27, 47]. Recently, we and other groups have reported critical roles for sub-cellular ROS balance for optimal EC viability and proliferation [1–3, 8, 50].

An emerging approach to study EC biology is to modulate sub-cellular ROS levels [6, 50]. Our group has previously shown that a short-term endothelium-specific increase in ROS derived from NADPH oxidase 2 (NOX2) overexpression (OE) results in an increase in coronary vasodilation and in EC proliferation [49, 50]. This result

was linked with the activation of AMP kinase (AMPK) and endothelial NO synthase (eNOS), with a key increase in the activity of the mitochondrial isoform of superoxide dismutase (MnSOD) enzyme and consequent reduction of mito-ROS. In contrast, long-term OE of NOX2 and hence sustained ROS production resulted in EC dysfunction. Despite the activation of AMPK and eNOS in ECs with a prolonged increase in ROS levels, MnSOD activity decreased, thereby increasing mito-ROS [49, 50]. This difference in short-term versus long-term exposure to ROS and associated changes in mito-ROS levels underscore the importance of mito-ROS homeostasis to ECs. In fact, it has been previously reported that a lack of MnSOD increases mito-ROS leading to extensive mitochondrial injury, followed by neonatal dilated cardiomyopathy and subsequent death [32, 35]. These reports highlight that although ECs have a relatively low volume of mitochondria, their mito-ROS is of great importance for the pathophysiology of cardiovascular disorders, as previously reviewed by other groups [17, 71].

Whereas most cells in the body utilize oxidative phosphorylation to generate energy (ATP), ECs are unique in its dependence on extra-mitochondrial glycolysis for ATP synthesis [18]. Recent studies demonstrated that mitochondrial antioxidant MnSOD, by lowering the levels of mito-ROS, helps maintain an optimal balance between sub-cellular ROS and endothelial function in coronary vascular EC [8, 50]. However, it is not known whether regulated levels of EC-specific mito-ROS have any effects on ATP synthesis and resilience of coronary EC in post-MI ischemic myocardium.

Based on our and others' previous results, we hypothesized that rather than global and non-specific usage of antioxidants, use of endothelium-specific antioxidant aimed at modulating ROS at the subcellular level, i.e. mitochondria, may play crucial roles in EC homeostasis and may improve coronary angiogenesis in post-MI ischemic myocardium. In the present study, we tested this hypothesis by using a novel conditional binary transgenic mouse model that *O*ver-*E*xpresses MnSOD (MnSOD-OE) specifically in the mitochondria of ECs and evaluated coronary vascular density resulting in the recovery of post-MI cardiac function. Using this transgenic animal model, we report here that reduction in EC-specific mitochondrial oxidants induces coronary angiogenesis in post-MI hearts resulting in the recovery of cardiac function.

Materials and methods

An extended version of materials and methods is available in the Online Supplementary file.

Statement of data availability

All supporting data are available within the article and its online supplementary files. Raw data from this study are available from the corresponding author upon reasonable request.

Ethical statement

This study was approved by the Lifespan Institutional Animal Care and Use Committee of the Rhode Island Hospital, under protocol number 0093-16. All the ethical regulations were strictly followed as established by the Animal Welfare Act, the Public Health Service Policy on Humane Care and Use of Laboratory Animals, and the Guide for the Care and Use of Laboratory Animals. The manuscript does not contain clinical studies or patient data.

Generation of binary Tet-MnSOD:VE-Cadherin-tTA mice

The present study consisted of in vitro, *ex-vivo* and in vivo experiments using a novel double transgenic mouse model (Tet-MnSOD:VE-Cadherin-tTA) that presents conditional OE of MnSOD by a tetracycline (Tet) OFF system. The MnSOD-OE was restrained specifically in ECs, by the linkage of the tetracycline-controlled transactivator (tTA) to the vascular endothelial cadherin (VE-cadherin) gene promoter [49]. A summary of the transgenic model generation is available in Supplementary Fig. 1A-C. Shortly, Tet-MnSOD mice were generated and crossbred with VE-Cad-tTA, producing Tet-MnSOD:VE-Cad-tTA offspring, which was kept on Tet since in utero. The presence of Tet-MnSOD:VE-Cad-tTA genes was confirmed by *Polymerase Chain Reaction (PCR).* A detailed description of the development of our novel transgenic model is available in the online Supplementary file.

Animal genotyping by polymerase chain reaction (PCR)

To identify double-positive Tet-MnSOD:VE-Cad-tTA transgenic mice, DNA was isolated from 8–9 days-old mice tail snips and PCR was carried out using Platinum® PCR Supermix (Invitrogen, Carlsbad, CA). DNA was isolated using the Hot Sodium Hydroxide and Tris method [59] and amplified by a programmable thermal cycler (Bio-Rad C1000 Touch Thermal Cycler, Bio-Rad Laboratories, Inc., Hercules, CA). The amplified PCR products were separated via gel electrophoresis. PCR product bands were visualized under short-wave UV light, and photos were taken using a gel documentation system (G-Box Chemi XT16, Syngene, Frederick, MD). VE-Cadherin gene was detected using the primers: tTA_S1:5′-GACGCCTTAGCCATTGAGAT-3′

and tTA_A1 5′-CAGTAGTAGGTGTTTCCCTTTCTT-3′, whereas MnSOD was detected by Tet_S1: 5′-AGAGAA AAGTGAAAGTCGAGCTCGGT-3′ and Tet_SOD_A1: 5′-TTAGGGCTCAGGTTTGTCCAGAAAAT-3′ (Integrated DNA Technologies Inc., USA). Only the animals that had confirmed the presence of both VE-cadherin and MnSOD genes were used in the study.

In vitro and ex vivo studies

Quantitative real-time assessment of angiogenesis, endothelial and mitochondrial function in a living animal in vivo can sometimes be challenging. For this reason, in addition to in vivo cardiac function measurements (echocardiogram) in the non-reperfused MI model, ECs were isolated and several ex vivo and in vitro assays were carried out as described in the sections below. EC mitochondria activity by seahorse and native gel (for supercomplex formation assays) were studied in vitro. We also performed wound healing assay in vitro and aortic sprouting ex vivo, as a functional measure of EC migration and angiogenesis, respectively; both are recognized ex vivo and in vitro methods to measure the angiogenic potential of EC. Proteomic and other assays were also performed. Together, the in vivo, in vitro and ex vivo results presented in this study provide a better understanding of molecular mechanisms by which genetic modulation of mito-ROS induce functional and phenotypic changes in EC.

Isolation of MHECs from MnSOD mice

Due to the lack of quantitative EC-specific superoxide formation and MnSOD activity assays in vivo or in intact cardiac tissue, mouse heart ECs (MHEC) were isolated and subject to several quantitative assays in vitro. To that end, hearts were harvested from 10 to 14-day-old mice ($n = 3$/group for each isolation). After collagenase treatment, mouse heart ECs (MHEC) were incubated with sheep anti-rat IgG Dynabeads (Life Technologies, USA) and rat anti-mouse CD31 (BD Pharmingen™, USA), followed by magnetically activated cell sorting, as previously described [49]. The isolated cells were cultured and used from passages 1 to 2. All experiments in this study represent results from 6 different isolations, each individual experiment was performed at least two times. AcLDL incorporation and VwF immunofluorescence qualitative analyses were performed to confirm the purity of isolated ECs (Supplementary Fig. 2).

Tetracycline treatment for conditional MnSOD OE in EC

For the in vitro and *ex-vivo* studies, the tetracycline was added to the medium (2 µg/ml) of the control cells (Tet-ON) to prevent the OE of MnSOD, meanwhile Tet-OFF cells (OE group) received only the medium with vehicle (Saline). The medium was replaced every 48 h and always prepared with fresh tetracycline/saline.

For the in vivo study, tetracycline (2 mg/ml) was mixed with the drinking water (light-blocking water bottle) of Tet-ON groups to prevent the OE of MnSOD in ECs, while the Tet-OFF group received just the vehicle (drinking water). The tetracycline/vehicle water was changed every week [49, 50].

Oxidative status measurements

EC Immunofluorescence—MHECs were allowed to grow until 80% confluency and then processed for immunofluorescence of MnSOD, following the manufacturer's protocol (Cell signaling Technology, USA). Slides were imaged at 20× objective on an upright microscope (Eclipse E800, Nikon Instruments Inc., USA) using spot Advanced™ Software (SPOT Imaging, USA).

Live-cell mitochondria and mitochondrial ROS fluorescence—MHEC were cultured to 80% confluency. Cells were thereafter incubated with 100 nM MitoTracker® Green FM to label mitochondria, and 5 µM MitoSOX™ fluorescent probe to estimate mitochondrial ROS production, following the manufacturer's protocol (Thermo Fisher Scientific, USA) [50]. Each well was imaged at 20× objective on an inverted microscope (Eclipse Ts2, Nikon Instruments Inc., USA). Mitochondrial ROS fluorescence was also measured on a 96-well plate reader after labeling with MitoSOX.

Mito-roGFP assay—Mito-roGFP assay was performed as previously described [56]. Imaging was performed using a Nikon ECLIPSE TE20000-U microscope (Nikon Instruments Inc., NY, USA) with excitation and emission filters at 405/488 nm. The oxidative status was then quantified considering the maximal reduction and oxidation.

Assessment of angiogenesis by scratch and aortic sprouting assay

Scratch/wound healing assay—MHECs at passage 2 were cultured to confluency. The scratch was performed using a 200 µl pipet tip and the cells were immediately imaged (time 0), followed by consecutive imaging at 6 h, 12 h, and 24 h after the wound at 4× magnification in an inverted microscope (Eclipse Ts2, Nikon Instruments Inc., USA). The percent of wound closure was quantified by ImageJ (NIH, USA) [16].

Aortic sprouting—Aortae were harvested from mice and kept in ice-cold 1× DPBS during the cleaning procedure in a sterile 10 cm plate. After cleaning, each aorta was cut into 6–8 1 mm ring sections. Each ring was placed into one well in a 96-well plate pre-coated with Cultrex Basement membrane extract (BME). Additional BME solution was placed

on top, followed by culture medium with or without tetracycline. Cells were allowed to sprout and imaged 4 days after plating. Sprouting was analyzed using angiogenesis software Angiotool [72].

Protein expression analysis by Western Blot

Western blot was carried out using XCell *SureLock*® Mini-Cell system with NuPAGE® 4–12% Bis–Tris (denaturing, reducing) gels (ThermoFisher Scientific, USA). Bands were obtained and imaged by enhanced chemiluminescence method using ChemiDoc XRS + (Biorad, USA) [50].

Proteomics

MHEC were isolated from 10- to 14-day-old mice ($n = 4$ mice/group) and cultured with (Tet-ON; Control) or without tetracycline (Tet-OFF; MnSOD-OE) until passage 2. MHEC were gently washed with 1× DPBS, trypsinized, centrifuged for 5 min at 1000 rpm, 4 °C, followed by 4 washes with 1× DPBS. Cell pellets were homogenized for 2 min at 5.5 m/s speed by Bead ruptor Elite (Kennesaw, GA) with a lysis buffer (8 M urea, 1 mM sodium orthovanadate, 20 mM HEPES, 2.5 mM sodium pyrophosphate, 1 mM β-glycerophosphate, pH 8.0, 20 min, 4 °C) and cleared by centrifugation (14,000×*g*, 15 min, 15 °C). A total of 100 µg of protein per sample was subjected to in-solution trypsin digestion. Tryptic peptides were desalted using C18 Sep-Pak plus cartridges (Waters, Milford, MA) and were lyophilized for 48 h to dryness. The dried peptides were reconstituted in 100 µl of buffer A (0.1 M acetic acid) and 2 µg was injected for each analysis. The LC–MS/MS was performed on a fully automated proteomic technology platform that includes an Agilent 1200 Series Quaternary HPLC system (Agilent Technologies, Santa Clara, CA) connected to a Q Exactive Plus mass spectrometer (Thermo Fisher Scientific, Waltham, MA) as described earlier [5]. MS raw files were searched against the Uniprot Mus musculus database (TaxonID: 10090, downloaded on 02/09/2015) using the Sequest algorithm within Proteome Discoverer v 2.3 software (Thermo Fisher Scientific, San Jose, CA). The Sequest database search was performed with the following parameters: trypsin enzyme cleavage specificity, 2 possible missed cleavages, 10 ppm mass tolerance for precursor ions, 0.02 Da mass tolerance for fragment ions. Search parameters permitted dynamic modification of methionine oxidation (+ 15.9949 Da) and static modification of carbamidomethylation (+ 57.0215 Da) on cysteine. Peptide assignment from the database search was filtered down to a 1% FDR. The relative label-free quantitative and comparative among the samples were performed using the Minora algorithm and the adjoining bioinformatics tools of the Proteome Discoverer 2.3 software. To select proteins that show a statistically significant change in abundance between two groups, a threshold of 1.5-fold change with p value (< 0.05) were selected.

Mitochondrial oxygen consumption by Seahorse

MHEC were plated in 0.1% (w/v) gelatin-coated Seahorse XFe96 V3 PS cell culture microplates (2.0×10^4 cells per well). Mitochondrial oxygen consumption rates (OCR) were measured in the next day using Agilent Seahorse XFe96 Analyzer according to the manufacturer's protocol (Agilent Technologies, Wilmington, DE). Briefly, a hydrated sensor cartridge was loaded in its injection ports with oligomycin, carbonyl cyanide-p-trifluoromethoxyphenylhydrazone [FCCP], and a mix of rotenone and antimycin A, respectively. Seahorse XF DMEM Medium (pH 7.4, Aligent) supplemented with 10 mM glucose, 1 mM pyruvate, and 2 mM L-glutamine (Sigma) was used as an assay medium. After the assays, cells were stained with Hoechst 33342 (1 µg/ml, Thermo-Fisher) for 30 min at room temperature protected from light and fluorescent signals were measured with excitation/emission at 350/460 nm using a plate reader SynergyMx (BioTek) for cell number normalization [37, 62, 68].

Mitochondrial membrane potential

Mitochondrial membrane potential ($\Delta_\psi m$) was estimated based on TMRE fluorescence, using the TMRE-Mitochondrial Membrane Potential Assay Kit (Abcam) in cells adhering to a 96-well clear bottom black side plate. Fluorescence was measured in a microplate reader at 549 ± 9 nm excitation and 575 ± 9 nm emission and used to estimate the mitochondrial membrane potential [50].

Mitochondria isolation and Blue Native-PAGE

MHECs were isolated using Dynabeads as described above (under 'Isolation of MHEC from MnSOD mice') ($n = 3$/group for each isolation) and cultured at passage 3 in T-175 3-layer flasks until 80% confluency. MHECs were collected by gentle trypsinization followed by mitochondria isolation using a kit from Thermo Fisher (cat# 89874) and following the manufacturer's protocol. Cells were lysed by performing 80 strokes with a Dounce homogenizer. Each flask contained MHEC isolated from 3 hearts and was treated as one individual sample. Mitochondrial pellet was resuspended in 200 µl of aminocaproic acid buffer and protein concentration was measured by BCA using a kit from Thermo Fisher (cat# 23235). BN-PAGE protocol was performed as described by Jha and collaborators [29], loading 20 µg of each sample. The proteins were transferred to a PVDF membrane by overnight wet transfer (20 h at 30 V). The following antibodies were tested: Total anti-OXPHOS rodent antibody

cocktail (Abcam cat# ab110413). Individual complexes and supercomplexes were identified by molecular weight based on NativeMark unstained protein standard (ThermoFisher cat# LC0725). An SDS-Page was performed using an equal amount of protein in parallel and an anti-VDAC antibody (Cell signaling cat# 4661) was used as a loading control.

In vivo study

Age and sex-matched mice were divided into control and OE group ($n = 10$–12/group). Control group (Tet-ON) received Tetracycline (2 mg/ml) in the drinking water to inhibit transgenic expression while MnSOD-OE group (Tet-OFF) received just the vehicle (drinking water) for 5 ± 1 weeks. At age 8 ± 1 week, both groups were subjected to echocardiography (Baseline assessment), followed by left anterior descending coronary artery (LAD) ligation surgery (permanent ligation, without reperfusion) on the next day (both procedures were conducted under appropriate anesthesia). Echocardiography was also performed on the 10th and 28th day after the non-reperfusion surgery ($n = 8$/group). After the final echocardiography (at age 12 ± 1 weeks), each mouse was anesthetized with a single overdose of Ketamine (200 mg/kg) and Xylazine (10 mg/kg) by intraperitoneal injection, followed by heart harvest. Echocardiography was also performed in equivalent timepoints for Tet-ON ($n = 6$) and Tet-OFF ($n = 6$) animals that did not undergo surgery.

Permanent LAD Ligation and induction of non-reperfused MI

A permanent LAD ligation was performed as previously described by our and other groups, to induce a non-reperfused MI [30, 46]. Animals received a combination of Ketamine (50 mg/kg, i.p.) and 3% isoflurane (via Vetflo vaporizer (Kent Scientific Corporation, USA) to induce anesthesia. When deeply anesthetized, the mouse was intubated (dorsal decubitus position) with a 20-gauge tracheal catheter cap and connected to a MiniVent ventilator (Harvard Apparatus, USA) under 2% isoflurane, 1.5 ml/min oxygen flow, 130 strokes/minute, 150 µl/stroke. A medial incision was made below the axillar level, followed by muscle layer retraction, an incision in the third intercostal space and the placement of a thorax retractor. The pericardium was gently removed, and the LAD was located and permanently sutured to induce a non-reperfused MI, by use of an 8–0 suture line. The intercostal space was then closed (6–0 suture line) and the pneumothorax removed/deflated, if any. Anesthesia was decreased to 1% while suturing skin to allow proper recovery of spontaneous breathing. Animal was then removed from the ventilator. Post-surgical care consisted of a single injection of slow-release Buprenorphine (1 mg/kg, s.c.). The cages were kept warm (37 °C) and recovery was monitored for 3 days following surgery. For SHAM mice, the same procedures were followed, but the suturing of the LAD was not performed.

Echocardiography

Transthoracic echocardiography was performed before LAD ligation surgery (Baseline), and at 10 and 28 days after non-reperfused MI surgery ($n = 8$/group), using Vevo 2100 ultrasound system (FUJIFILM VisualSonics Inc., Canada) and MS-550D transducer. Echocardiography results for ejection fraction (EF), fractional shortening (FS), fractional area change (FAC), end-systolic (ESV) and end-diastolic volumes (EDV), systolic (SAWT) and diastolic anterior wall thickness (DAWT), and systolic (SPWT) and diastolic posterior wall thickness (DPWT) were obtained as previously described [42, 57]. Echocardiography was also performed at equivalent time points for Tet-ON ($n = 6$) and Tet-OFF ($n = 6$) animals that did not undergo surgery, for wild-type FVBs ($n = 6$) that underwent SHAM surgery ($n = 5$), and for wild-type FVBs that underwent LAD ligation surgery and were treated (+Tet, $n = 6$) or not (−Tet, $n = 5$) with tetracycline.

Histology and immunofluorescence

Preparation of tissue sections—Each heart was embedded in Sakura Tissue-Tek O.C.T. Compound (Sakura Finetek, Torrance, CA, USA) immediately after harvesting. The tissues were cut into 5 µM thick sections in a cryostat and fixed in positively charged glass slides.

Masson's Trichrome staining—The heart sections were stained to verify collagen fibers by the Masson's Trichrome method, using a commercial kit (Polysciences Inc., USA) [39]. The slides were imaged at 1× objective on an upright microscope (Eclipse E800, Nikon Instruments Inc., USA). Images were used to measure MI area on ImageJ software (NIH) using previously described methodology [55].

Immunofluorescence—Heart sections were immunostained for MnSOD and anti-CD31 for confirmation of MnSOD-OE in vivo. Heart sections were also immunostained using proliferating cell nuclear antigen (PCNA) and anti-CD31 for EC proliferation, and anti-CD31 and anti-α-smooth muscle actin (αSMA) antibodies for capillary and arteriole density, followed by anti-Rat Alexa Fluor® 488 Conjugate secondary antibody and anti-Rabbit Alexa Fluor® 594 Conjugate secondary antibody [48]. DAPI was co-stained as a nuclear label. Microscopy was performed (Eclipse E800 upright microscope, Nikon Instruments Inc., USA) and the Spot Advanced™ Software (SPOT Imaging, USA) was used to capture images at either 20×, 40× or 60× objective. Colocalization was analyzed by JaCoP plugin on ImageJ software (NIH, USA). Percent of proliferating ECs

was manually counted, while capillary and arteriole density were quantified by particle analysis on ImageJ software. Immunofluorescence was also performed in heart sections of Tet-ON ($n=3$) and Tet-OFF ($n=3$) control animals that did not undergo surgery, for assessment of baseline capillary level.

Statistical analysis

Statistical analysis was carried out in GraphPad Prism 9. Normality of data was tested by Shapiro–Wilk's test. Data comparing two groups were tested by Student's *t* test. Parametric data comparing three groups were analyzed by One-Way ANOVA followed by Tukey's post hoc. Non-parametric data comparing three groups were analyzed by Kruskal–Wallis test and Dunn's post hoc. Data comparing four groups were statistically analyzed by Two-Way ANOVA and Tukey's post hoc. Time-lapse results were statistically analyzed by Mixed ANOVA followed by Sidak's multiple comparisons test. *p* values inferior to 0.05 were taken as significant. Results are shown as mean ± standard error of the mean (SEM).

Results

EC-specific OE of MnSOD decreases mitochondrial ROS

We have generated a novel binary conditional transgenic animal model that overexpresses mitochondrial antioxidant MnSOD in an EC-specific manner (Supplementary Fig. 1A–C). Expression of the HA-tagged MnSOD transgene in coronary EC was confirmed by co-localization of anti-HA and anti-CD31 (EC marker) antibodies in heart sections of MnSOD-OE animals (Supplementary Fig. 1D). Colocalization of CD31 and MnSOD in heart sections using immunofluorescence (Supplementary Fig. 1E) demonstrated that Tet-OFF group had 2 ± 0.4-fold increased colocalization compared to Tet-ON control (0.65 ± 0.13 in Tet-OFF versus 0.30 ± 0.03 in Tet-ON). To further confirm MnSOD OE in ECs, MHECs were isolated from MnSOD animal hearts and were subject to immunofluorescence using anti-MnSOD and anti-HA antibodies. MHECs from Tet-OFF animals showed 1.7 ± 0.2-fold increase in MnSOD fluorescence compared to MHEC from Tet-ON animals (1.68 ± 0.59 in Tet-OFF versus 1.00 ± 0.30 in Tet-ON; Fig. 1A). Western blot analysis using anti-HA antibody showed expression of the transgene HA-MnSOD only in the protein lysates of MHEC from Tet-OFF animals but not Tet-ON animals (Fig. 1B). Western blot analysis using MHEC protein lysates demonstrated a significant increase (by 1.3 ± 0.04-fold) in the expression of MnSOD in MHECs from MnSOD-OE compared to control MnSOD (14.26 ± 0.83 in Tet-OFF versus 10.74 ± 1.1 in Tet-ON, Fig. 1C). This OE of MnSOD was accompanied with 50% decrease in mito-ROS in MHEC from Tet-OFF compared to Tet-ON MHECs as determined by mitoSOX assays (0.460 ± 0.22 in Tet-OFF versus 1.00 ± 0.35 in Tet-ON, Fig. 1D and Supplementary Fig. 3). To further confirm mitochondria-specific reduction in ROS, adenovirus-based Mito-roGFP ratiometric analysis of oxidation/reduction was performed as described (Material and Methods) [56]. Figures 1E-F show a 21% reduction in oxidation in MHECs from Tet-OFF (18.36 ± 0.87% oxidized) compared to Tet-ON (23.11 ± 0.76% oxidized), confirming a significant reduction in mito-ROS by MnSOD transgene expression in EC.

EC-specific MnSOD-OE improves left ventricle function in non-reperfused MI

To examine the effects of a reduction in mito-ROS on coronary EC, the binary transgenic MnSOD mice were subject to non-reperfused MI as described before [46]. We evaluated baseline (day 0), and post-MI cardiac function (at day 10 and day 28) using left ventricular echocardiography. The hearts were harvested after 28 days of MI, and heart sections were subject to Masson's trichrome staining to determine the infarct size (collagen deposition). A 27% reduction in infarct areas were observed in MnSOD-OE (23.21 ± 6.66%) as compared to control (30.36 ± 4.66%) hearts 28 days post-infarction (Fig. 2A). The echocardiographic assessment revealed a 16% improvement in ejection fraction (EF, 56.03 ± 3.79 in Tet-OFF versus 48.13 ± 4.73 in Tet-ON) and 20% increase in fractional shortening (FS, 28.76 ± 2.71 in Tet-OFF versus 24.02 ± 3.21 in Tet-ON) of Tet-OFF as compared to Tet-ON mice (Fig. 2B). MnSOD-OE mice also demonstrated significantly improved recovery in EF (10.65 ± 9.30% in Tet-OFF versus − 12.98 ± 12.70% change in Tet-ON) and FS (18.34 ± 14.59% in Tet-OFF versus − 11.52 ± 12.76% change in Tet-ON) during the period between 10- and 28-days post-MI (Fig. 2C). Additional comparison between Tet-ON and Tet-OFF at the baseline (before MI surgery) and between baseline and endpoint (day 28 post-MI) echocardiographic assessments are presented in Supplementary Tables 1 and 2. There were no significant baseline (pre-MI) differences observed in EF and FS among the groups (Tet-ON vs Tet-OFF). Representative videos of baseline (before MI) and endpoint (28 days after non-reperfused MI) echocardiography are shown in Supplementary video 1. Comparison between MnSOD-OE Tet-ON and Tet-OFF non-infarcted animals versus Tet-ON/Tet-OFF infarcted mice are shown in Supplementary Fig. 4 and Supplementary video 2. To examine whether tetracycline alone has any effects on the recovery of non-reperfused MI cardiac function, additional comparison between wild-type SHAM versus wild-type +Tet (with tetracycline) and −Tet (without tetracycline)

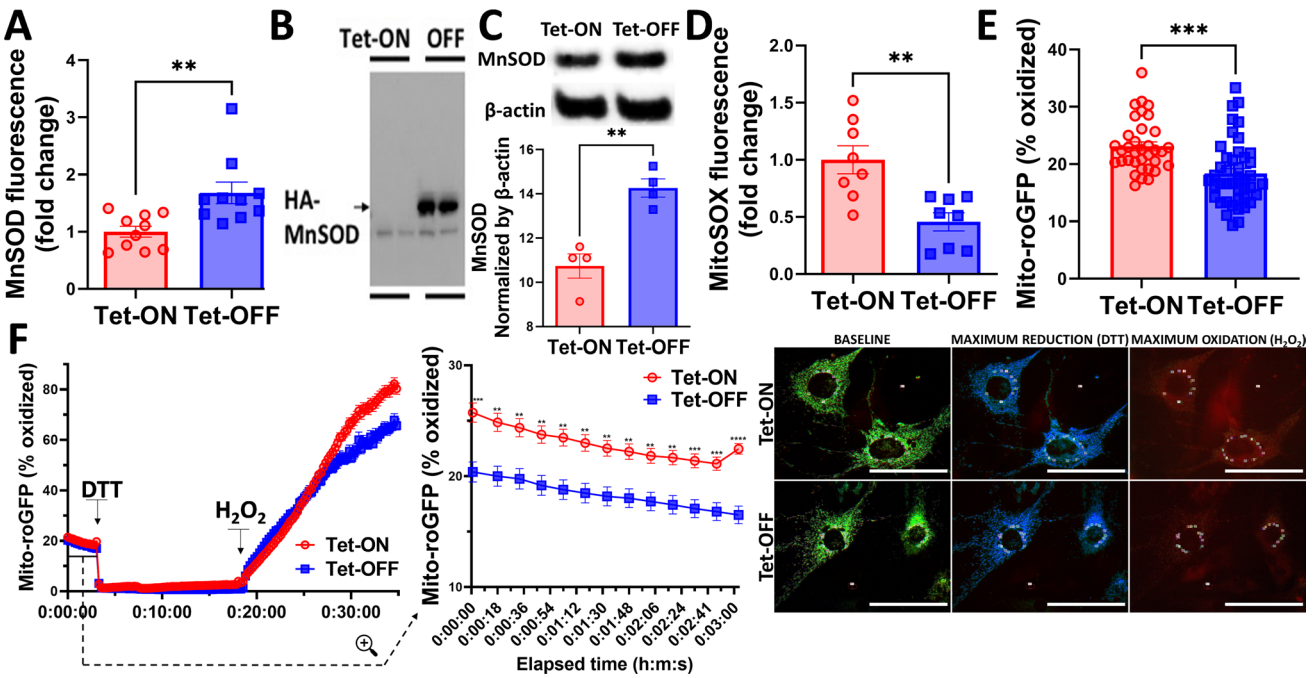

Fig. 1 Endothelium-specific MnSOD OE in a novel binary conditional transgenic mouse model demonstrates a significant reduction in mitochondrial ROS in MHEC. **A** Quantitative analysis of MnSOD fluorescence demonstrates 1.7 ± 0.2-fold increase in Tet-OFF (MnSOD-OE) MHEC compared to Tet-ON (Control) MHEC. Isolated MHEC were immunoassayed using anti-MnSOD antibody and imaged in the upright microscope for measurement of fluorescence intensity. Representative immunofluorescence images of MnSOD are shown in Supplementary Fig. 2E. **B** Western blot analysis of MHECs from two independent transgenic animal lines using anti-HA antibody shows HA-tagged MnSOD transgene expression in Tet-OFF but not in Tet-ON mice. **C** Western blot analysis using purified MHEC protein lysates shows 1.3 ± 0.04-fold increase in MnSOD expression in Tet-OFF compared to Tet-ON MHEC. Representative images (upper panel) and quantitative analysis (lower panel) of Western blots are shown. **D** Mito-ROS content was significantly reduced in Tet-OFF MHEC (by 50%) compared to Tet-ON MHEC as measured using MitoSOX red probe in a spectrofluorometer (see Materials and Methods). Colocalization analysis of ROS and mitochondria were carried out using microscopy of mitoSOX and Mitotracker stained MHECs as shown in Supplementary Fig. 3B. **E** Quantitative analyses and **(F)** representative images showing percent (%) changes in mitochondrial ROS level using Mito-roGFP probe as a measure of mitochondrial oxidant contents in Tet-ON and Tet-OFF MHEC. Statistical analyses were carried out using two-tailed unpaired Student's *t* test (**A**, **C**, **D**, **E**) or by Mixed ANOVA followed by Sidak's multiple comparisons test for time-lapse results (**F**). $n = 10$/group for Immunofluorescence (**A**), $n = 4$/group for Western blot results (**C**), $n = 8$–11/group for MitoSOX fluorescence (**D**), and 39–44 ROIs from two different plates of MHEC, isolated from three individual hearts/group (**E** and **F**). Scale bar represents 100 µm. $^{*}p < 0.05$; $^{**}p < 0.01$; $^{***}p < 0.001$; $^{****}p < 0.0001$. *Tet-ON* MnSOD Control, *Tet-OFF* MnSOD-OE

infarcted animals were carried out. There were no significant differences in the post-MI cardiac function between +Tet and −Tet animals (Supplementary Fig. 5), further confirming the improvement in infarct size (Fig. 2A) and post-MI cardiac function observed in Tet-OFF animals (Fig. 2B) were due to overexpression of the transgene MnSOD in EC.

MnSOD-OE animals have increased coronary capillary and arteriolar density in the post-MI ischemic region

Next, using the non-reperfused MI model, we examined whether improvement in post-MI cardiac function in MnSOD-OE animals was associated with an increase in coronary capillary and arteriolar vessel density in the infarcted regions. Immunofluorescence using anti-CD31 and anti-αSMA antibodies on frozen heart sections (28 days post-MI) demonstrated that Tet-OFF animals had significantly increased the number of capillaries (by 3.4 ± 0.9 fold; 5.33 ± 4.51 in Tet-OFF versus 1.00 ± 0.55 in Tet-ON) and arterioles (by 5.0 ± 0.8 fold; 4.97 ± 2.08 in Tet-OFF versus 1.00 ± 0.99 in Tet-ON) in ischemic areas compared to Tet-ON animals (Fig. 3A and B). Interestingly, heart sections from the non-ischemic areas of the left ventricle (LV) of Tet-OFF animals also showed significantly increased coronary capillary density compared to Tet-ON animals (4.83 ± 4.05 in Tet-OFF versus 1.00 ± 0.24 in Tet-ON, Supplementary Fig. 6A-B). We then examined whether increased coronary vascular density in post-MI MnSOD-OE hearts was either due to increased survival of the existing vessels or due to new vessel formation (e.g. coronary angiogenesis). PCNA, a marker of active cell proliferation, and CD31 co-immunofluorescence analysis of frozen heart sections demonstrated an increase in EC proliferation (by 2.4 ± 0.9 fold; 19.09 ± 2.53

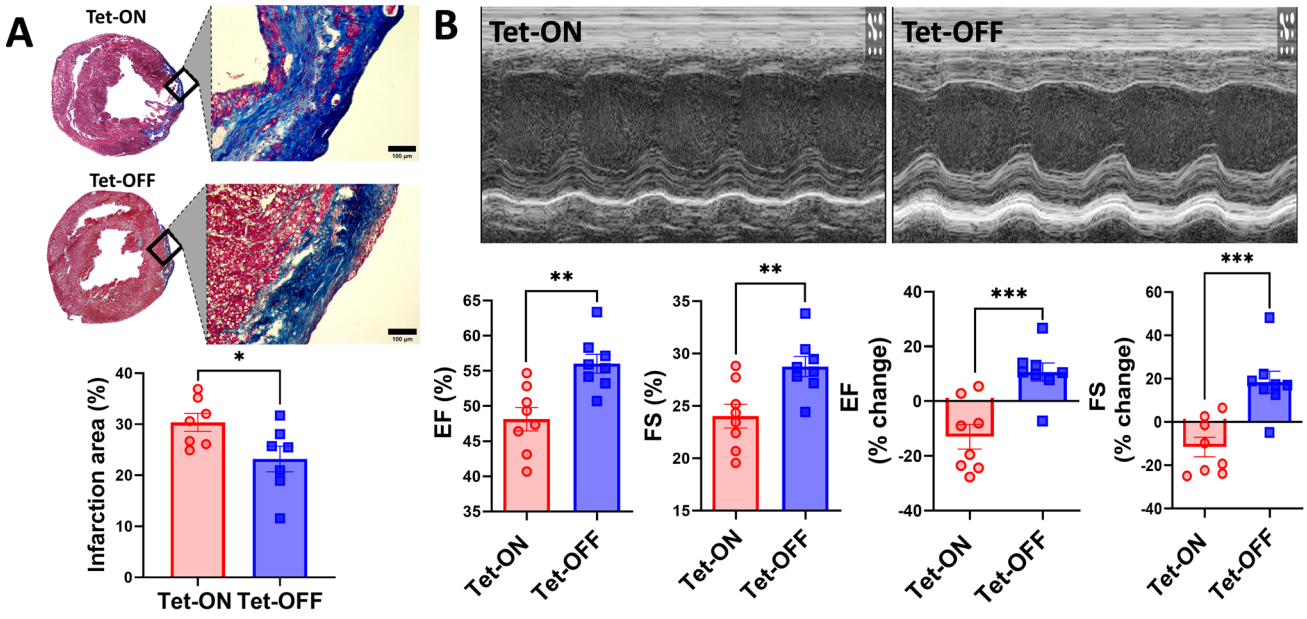

Fig. 2 Endothelium-specific MnSOD-OE improves cardiac function after non-reperfused MI. **A** Representative trichrome images of Tet-ON and Tet-OFF mice hearts (upper panel) 28 days post-MI. Quantitative analysis shows a 27% reduction in the size of the infarcted myocardium in Tet-OFF hearts compared to Tet-ON animals (lower panel). **B** Representative images of M-Mode echocardiographic assessment at short-axis view of Tet-ON and Tet-OFF are shown (upper panel). Quantitative analysis of left ventricle EF and FS show significant improvement in MnSOD-OE animals after 28 days of non-reperfused MI (lower panel). **C** Significant percent changes in EF and FS from the 10th to the 28th day after MI in Tet-OFF versus Tet-ON animals are shown. Quantitative analyses were carried out using a two-tailed unpaired Student's *t* test. $n=7$/group (**A**); $n=8$/group (**B** and **C**). *$p<0.05$; **$p<0.01$; ***$p<0.001$. *Tet-ON* MnSOD Control, *Tet-OFF* MnSOD-OE

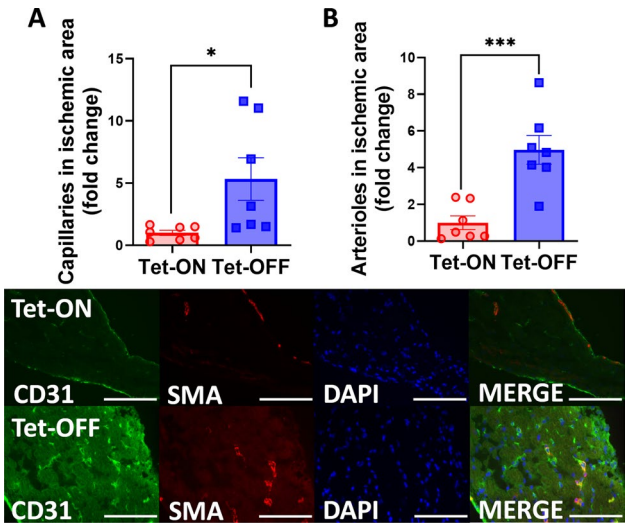

Fig. 3 Increased capillary and arteriole densities in non-reperfused ischemic myocardium of Tet-OFF compared to Tet-ON mice. Quantitative analysis of **A** capillaries and **B** arterioles in ischemic myocardium 28 days after permanent (non-reperfusion) LAD surgery are shown (fold-changes). Representative images of capillaries and arterioles in ischemic areas of Tet-ON and Tet-OFF myocardium are shown (lower panels). Statistical analyses were carried out using a two-tailed unpaired Student's *t* test. $n=7$ animals/group, each dot representing an average result from 3 different areas per 5 sections of each heart. Scale bar represents 100 µm. *$p<0.05$; **$p<0.01$; ***$p<0.001$. *Tet-ON* MnSOD Control, *Tet-OFF* MnSOD-OE

in Tet-OFF versus 13.65 ± 1.12 in Tet-ON) in ischemic LV areas of post-MI MnSOD-OE animals. Taken together, the increase in EC proliferation and coronary vascular density suggest that MnSOD-OE induced coronary angiogenesis in post-MI ischemic myocardium (Fig. 4A and B). Notably, EC proliferation did not change in non-ischemic myocardium in the infarcted animals (Fig. 4C and D). In age- and sex-matched Tet-ON and Tet-OFF animals that did not undergo MI surgery (non-infarcted), there was no difference in capillary density (Supplementary Fig. 7A), arteriolar density (Supplementary Fig. 7B), or coronary EC proliferation (Supplementary Fig. 7C). These results suggest that reduction in mito-ROS primes coronary endothelium to proliferate preferably during or after MI.

Reduction in mito-ROS induces aortic sprouting ex-vivo and improves wound-healing (scratch) assay in MHEC in vitro

To examine whether reduced mito-ROS by MnSOD-OE induces EC proliferation in other vascular beds/organs, we performed ex vivo aortic sprouting using aortic rings isolated from transgenic animals. ECs overexpressing MnSOD showed a 69% increase in branching index (1.69 ± 1.32 in Tet-OFF versus 1.00 ± 0.72 in Tet-ON)

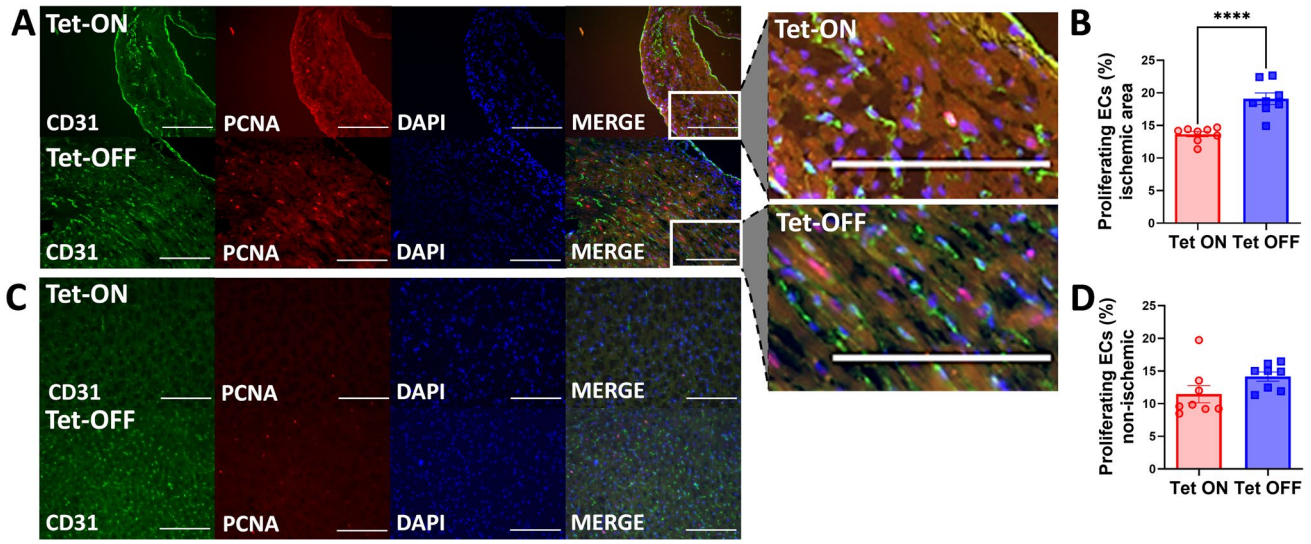

Fig. 4 Reduction in mitochondrial ROS by MnSOD-OE increases coronary EC proliferation in non-reperfused ischemic myocardium. **A** Representative images (left panel) and quantitative analysis (right panel) of percent of ECs undergoing proliferation (as determined by co-immunofluorescence of red PCNA and green CD31) in ischemic myocardium 28 days after non-reperfused MI. **B** Representative images (left panel) and quantitative analysis (right panel) of the percent of ECs undergoing proliferation (as determined by PCNA) in non-ischemic areas 28 days after non-reperfused MI. Statistical analyses and significance were determined by two-tailed unpaired Student's *t* test. $n = 8$ animals/group, each dot representing an average result from 3 different areas per heart section. Scale bar represents 100 µm. ****$p < 0.0001$. *Tet-ON* MnSOD Control, *Tet-OFF* MnSOD-OE

and 77% increase in total vessel length (1.77 ± 1.21 in Tet-OFF versus 1.00 ± 0.68 in Tet-ON) (Fig. 5A)), suggesting reduced mito-ROS may also induce EC proliferation in non-coronary vascular beds. Figure 5B shows a 28% increase in wound healing in MHECs from Tet-OFF (57.59 ± 7.62) compared to Tet-ON (45.08 ± 14.18), suggesting increased migration in ECs from MnSOD-OE. Together, these data suggest that EC-specific reduction in mito-ROS results in increased proliferation and migration of ECs.

MHECs from MnSOD-OE mice have significantly increased activation of Akt and ERK1/2 signaling pathways

To elucidate the effects of mito-ROS reduction on coronary EC, we performed Western blot analyses using protein lysates from MHECs and compared signaling pathway activation in Tet-OFF versus Tet-ON. Both Akt and Erk1/2 phosphorylation were increased by 80% (1.11 ± 0.29 in Tet-OFF versus 0.62 ± 0.09 in Tet-ON) and 49% (1.12 ± 0.17 in Tet-OFF versus 0.87 ± 0.17 in Tet-ON), respectively, in MHEC from Tet-OFF compared to Tet-ON (Fig. 6A and B and Supplementary Fig. 8). These findings suggest that MnSOD-OE induces activation of Akt and ERK1/2 signaling pathways in EC.

MnSOD-OE MHECs show increase in OXPHOS protein expression, TMRE fluorescence, and mitochondrial respiration

To better understand the mechanisms by which reduced mito-ROS helps ECs better cope and proliferate in ischemic myocardium, a comparative proteomic analysis using MHECs from Tet-OFF and Tet-ON hearts were performed. Detailed results of the label-free quantitative proteomic analysis are presented as PCA analysis, heat map clustering, and reactome pathway analysis (Supplementary Fig. 9A-B; Supplementary Excel files 1 and 2). A total of 4131 proteins were successfully identified and quantified, wherein 68 proteins were significantly increased (up-regulated) and 50 proteins were decreased (down-regulated) in abundance in MnSOD-OE sample compared to the control (Fig. 7A). KEGG analysis (https://string-db.org/) of these up-regulated proteins demonstrated that one of the major enriched pathways included the proteins associated with oxidative phosphorylation (OXPHOS) (Fig. 7B). Proteins associated with OXPHOS pathways such as COX6A1, NDUFA9, NDUFB1, NDUFV3, NDUVB3 and NDUVB7 showed twofold or higher increased abundance in MnSOD-OE ECs (Fig. 7C). A protein–protein interaction map of the up-regulated proteins further revealed a tight interaction and clustering of these proteins (Fig. 7D). This same cluster of proteins was identified by the Reactome analysis (https://string-db.org/)

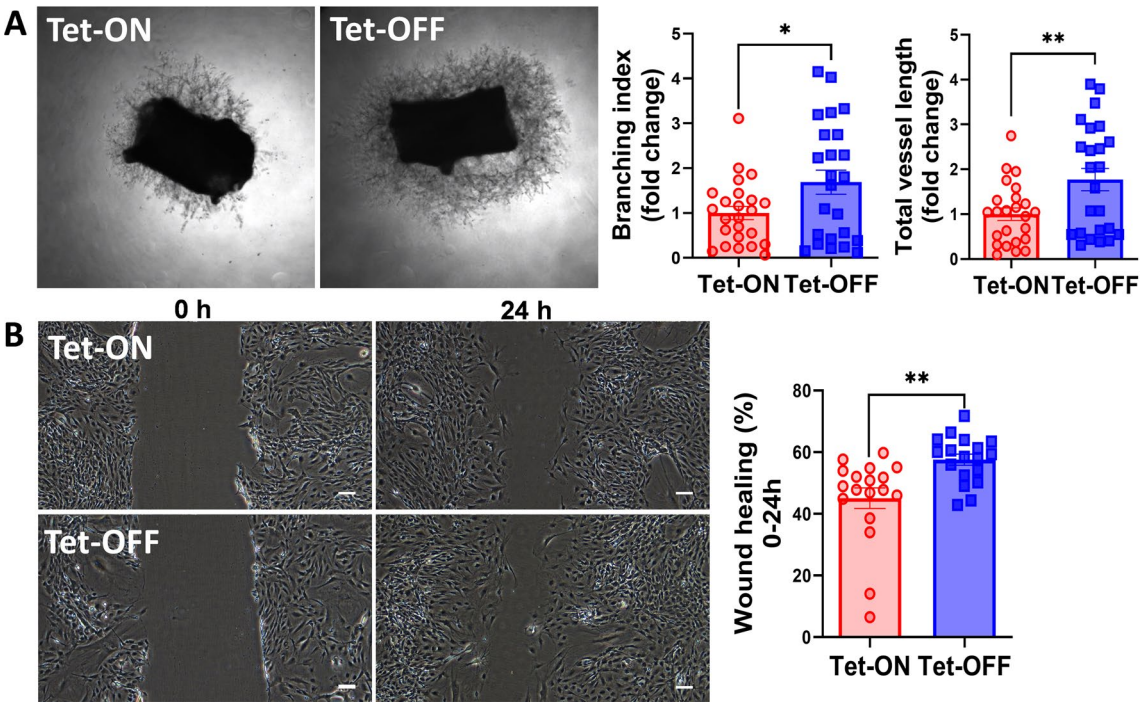

Fig. 5 MnSOD-OE stimulates aortic sprouting and MHEC migration. **A** Representative images (left panel) and quantitative analysis (right panel) of ex vivo aortic sprouting assay show increased branching index and vessel (sprout) length in Tet-OFF aortae compared to Tet-ON. **B** Representative images (left panel) and quantitative analysis (right panel) of in vitro wound healing (scratch) assay. Data from $n=6$ animals/group were analyzed using a two-tailed unpaired Student's t test. $n=23$ areas/group for aortic sprouting and $n=17$ areas/group for wound healing. Scale bar represents 100 µm. $^{*}p<0.05$; $^{**}p<0.01$. *Tet-ON* MnSOD Control, *Tet-OFF* MnSOD-OE

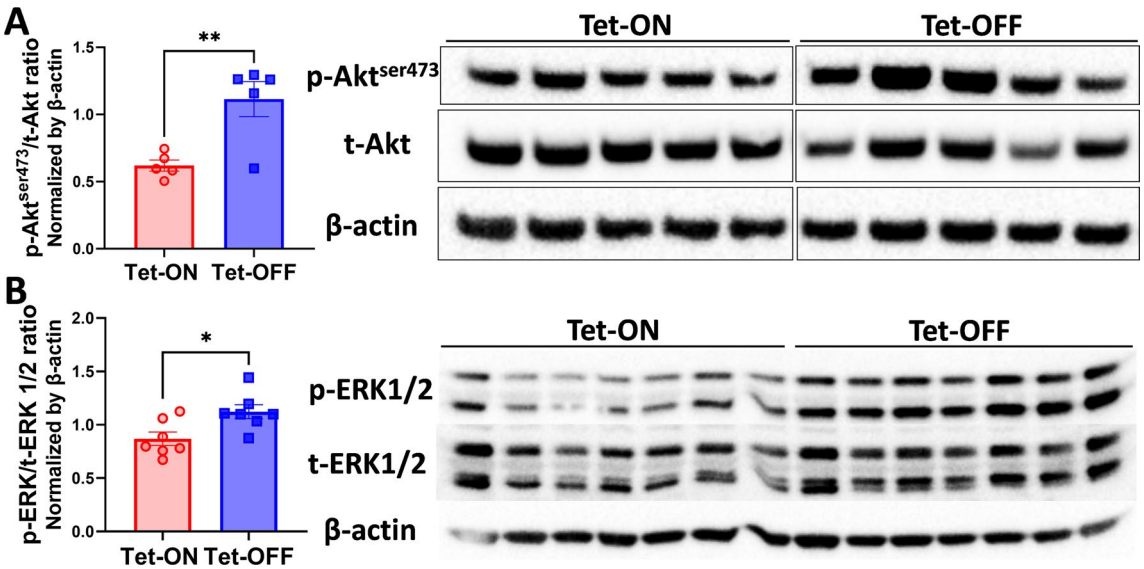

Fig. 6 MnSOD-OE activates Akt and ERK1/2 signaling pathways in MHEC. **A** Quantitative analysis of western blots using MHEC lysates from Tet-ON and Tet-OFF animals (left) and representative immunoblots (right panel) of phospho-Akt (p-Akt)/total Akt (t-Akt) ratio shows significant Akt activation in Tet-OFF MHEC. Bands were cut for easier visualization, as shown by the square around bands; the uncut western blot is available in the online supplemental file, Supplementary Fig. 6. **B** Quantitative results (left) and representative immunoblots (right panel) of phospho-ERK1/2 (p-ERK1/2)/total ERK1/2 (t-ERK1/2) ratio are shown. β-Actin was used as a loading control. Results were analyzed using a two-tailed unpaired Student's t test. $n=5$ MHEC isolation/group (**A**), $n=7$ MHEC isolation/group (**B**); 2–4 animal hearts were used for each MHEC isolation. $^{*}p<0.05$; $^{**}p<0.01$. *Tet-ON* MnSOD Control, *Tet-OFF* MnSOD-OE

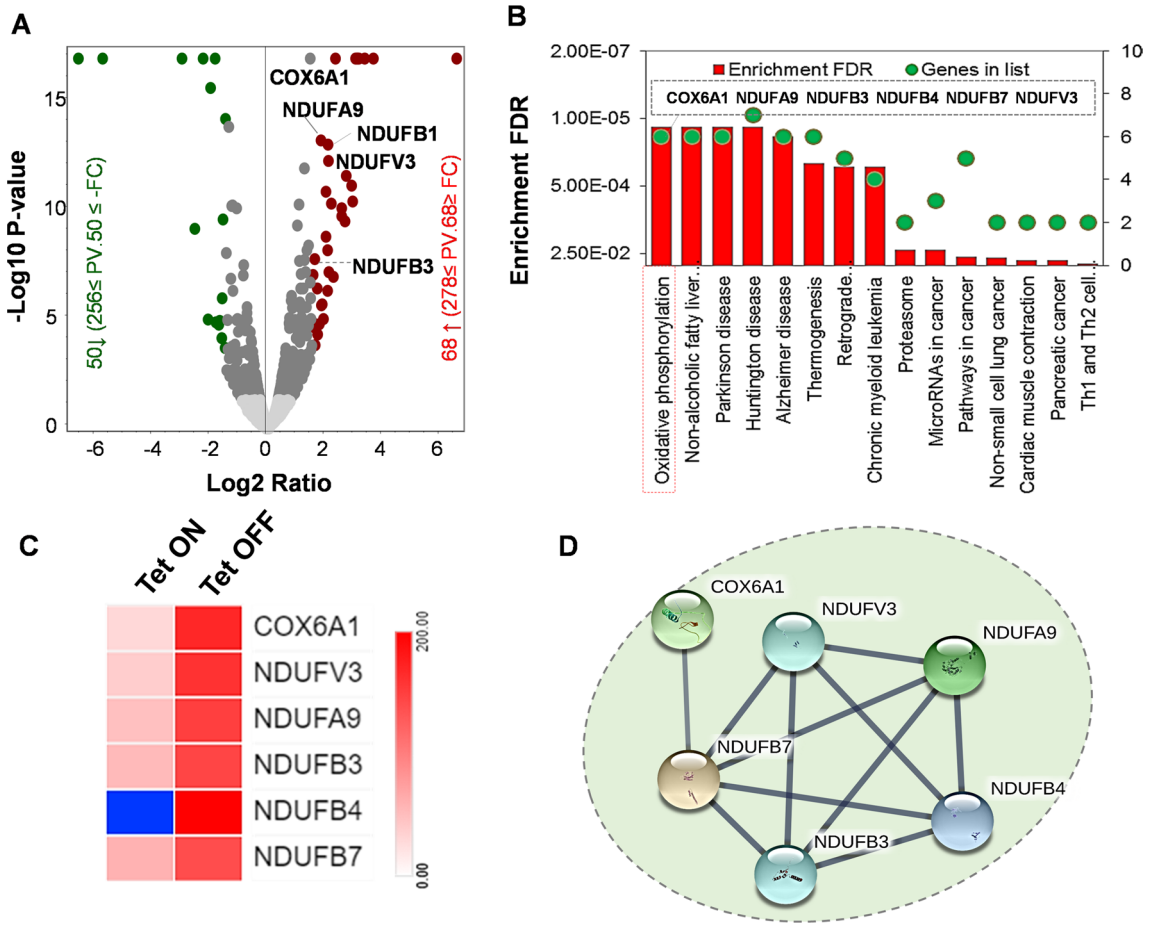

Fig. 7 Reduced mito-ROS increases OXPHOS signaling pathways in MHEC. **A** The volcano plot analysis of the significantly increased (red dot) and decreased (green dot) proteins in Tet-ON and Tet-OFF MHEC is shown. Gray dots are non-significant ($p=0.05$) and bellow the threshold fold-change (> 1.5 fold). **B** The KEGG pathway analysis of the up-regulated proteins. Red bar diagrams indicate the FDR enrichment and green circles indicate the number of proteins identified in each pathway. **C** Heat map shows the grouped ($n=3$) protein abundance of the targeted proteins. **D** Protein–protein interaction network of the proteins involved in oxidative phosphorylation. Line thickness indicates the strength of data support based on the experiments, co-expression, gene-fusion and co-occurrence data according to the STRING (https://string-db.org/). Statistical analysis was carried out by two-tailed unpaired Student's *t* test. $n=3$ replicates/group. $p<0.05$ was considered as statistically significant. *Tet-ON* MnSOD Control, *Tet-OFF* MnSOD-OE

as associated with mitochondrial Complex I biogenesis and respiratory electron transport chain (ETC) (Supplementary Fig. 9C).

To confirm the proteomic results, Western blot analysis was carried out using protein lysates from MnSOD-OE MHEC using an OXPHOS cocktail kit as described in Materials and Methods (Fig. 8A). There were significant increases in expression of mitochondrial ETC complexes I (0.96 ± 0.18 in Tet-OFF versus 0.50 ± 0.05 in Tet-ON, Fig. 8B) and IV (1.39 ± 0.07 in Tet-OFF versus 0.64 ± 0.02 in Tet-ON, Fig. 8E). No changes were found in the expression of mitochondrial complexes II (Fig. 8C), III (Fig. 8D), and V (Fig. 8F). These findings were accompanied with an increase in mitochondrial membrane potential (by 56%) in MnSOD-OE MHEC (24.32 ± 5.72 in Tet-OFF versus 15.59 ± 5.85 in Tet-ON) as estimated using TMRE fluorescence (Fig. 9A). With the increase in ETC complexes I and IV, and in mitochondrial membrane potential, we next wanted to examine the effects of reduced mito-ROS on MHEC OXPHOS using seahorse to measure OCR in the mitochondria of MnSOD-OE MHEC (Fig. 9B). Interestingly, MnSOD-OE MHEC showed significant increase in basal respiration (65.70 ± 1.14 in Tet-OFF versus 60.20 ± 1.48 in Tet-ON, Fig. 9C) and in ATP-linked respiration (63.64 ± 0.97 in Tet-OFF versus 49.12 ± 1.21 in Tet-ON, Fig. 9D), in addition to having 26% higher maximum respiration (133.04 ± 8.34 in Tet-OFF versus 105.84 ± 3.30 in Tet-ON, Fig. 9E) and 46% increase in spare respiration capacity (66.77 ± 9.05 in Tet-OFF versus 45.64 ± 3.18 in Tet-ON, Fig. 9F). There was no difference in proton leak or in non-mitochondrial oxygen consumption, as shown in Fig. 9G and H. Together, these findings suggest that reduction in mito-ROS increased mitochondrial ETC

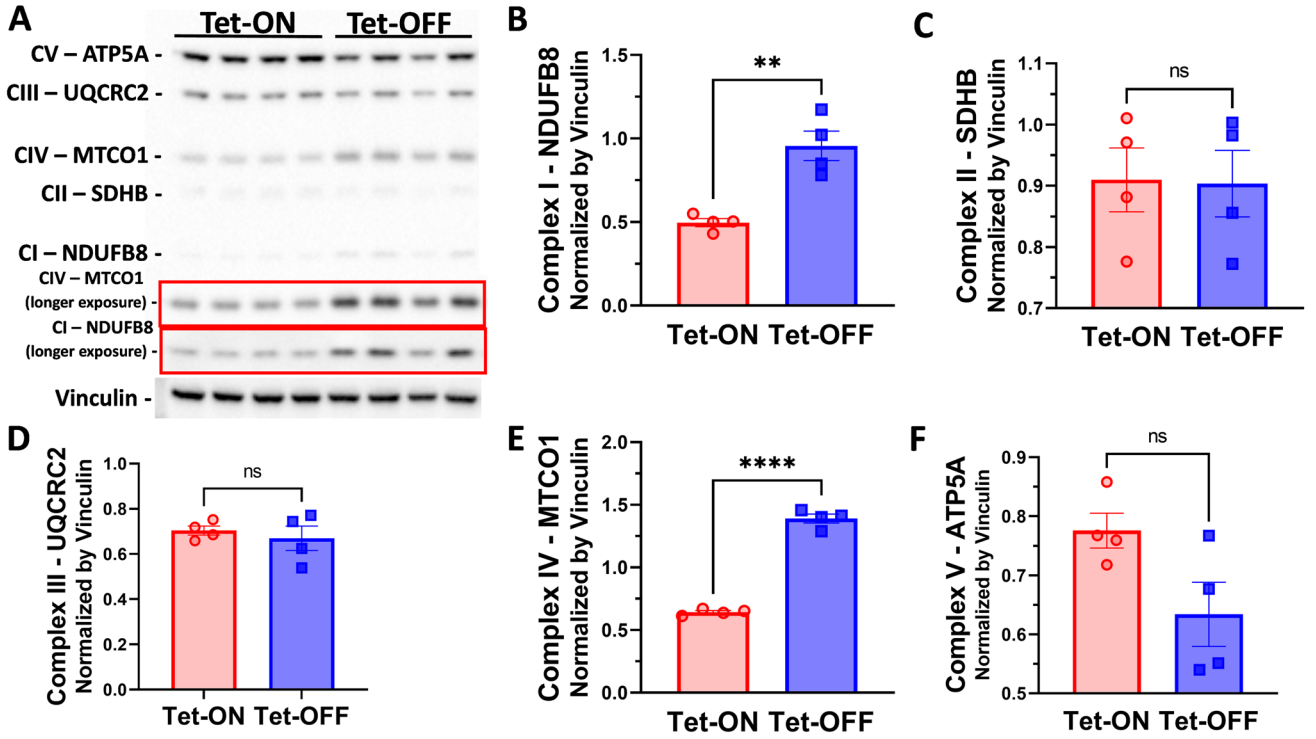

Fig. 8 MnSOD-OE increases expression of the mitochondrial complexes I and IV. **A** Representative western blot images of the individual mitochondrial complexes expression in Tet-ON and Tet-OFF MHEC lysates probed using OXPHOS rodent antibody cocktail kit (Abcam), and vinculin as the loading control. **B**–**F** Quantitative analyses of expression of mitochondrial complexes I—V. Statistical analysis was carried out by two-tailed unpaired Student's *t* test. $n = 4$/group. $^{*}p < 0.05$; $^{**}p < 0.01$; $^{****}p < 0.0001$. *Tet-ON* MnSOD Control, *Tet-OFF* MnSOD-OE

complexes expression and improved mitochondrial membrane potential resulting in increased OXPHOS in MnSOD-OE MHEC.

MnSOD-OE increases mitochondrial supercomplexes assembly in MHECs

We next evaluated whether the increased expression of mitochondrial complexes, increased mitochondrial membrane potential and respiration (OCR) could be associated with changes in the assembly of mitochondrial supercomplexes (SCs). A Native-PAGE western blot showed that MnSOD-OE increases the abundance of SC5 (1.37 ± 0.09 in Tet-OFF versus 0.48 ± 0.13 in Tet-ON), SC3 and SC2 (1.32 ± 0.06 in Tet-OFF versus 0.46 ± 0.08 in Tet-ON), and SCI (1.20 ± 0.04 in Tet-OFF versus 0.74 ± 0.09 in Tet-ON), as shown in Fig. 10A–D. Another supercomplex comprised of CV, CIII dimer and Complex IV was increased (1.52 ± 0.06 in Tet-OFF versus 0.89 ± 0.05 in Tet-ON) (Fig. 10E). Free complex I (1.48 ± 0.12 in Tet-OFF versus 0.54 ± 0.11 in Tet-ON) and CIV dimer (1.95 ± 0.11 in Tet-OFF versus 0.90 ± 0.09 in Tet-ON) were increased in MnSOD-OE MHEC mitochondria (Fig. 10F and G). Free CV was decreased in MnSOD-OE MHEC mitochondria (0.39 ± 0.01 in Tet-OFF versus 0.78 ± 0.10 in Tet-ON, Fig. 10H), which may be due to increased utilization of CV in the formation of supercomplexes in MnSOD-OE MHECs (Fig. 10A). There was no change in CIII dimer (Fig. 10I), CIII associated with CIV (Fig. 10J), free CIV (Fig. 10K), or free CII (Fig. 10L). These findings suggest that reduced mito-ROS in MHEC modulates the organization of mitochondrial supercomplexes, including an increase in the assembly of SC3 and SC2 (also known as respirasomes). These changes in SC formation by reduced mito-ROS plausibly allow for a more efficient ETC and increased OXPHOS in EC as evidenced in this study.

Discussion

This study addressed an interesting question of whether a reduction in mito-ROS in vascular endothelium, using genetic manipulation, modulate survival and proliferation of coronary ECs and induces coronary angiogenesis to recover cardiac function in an animal model of non-reperfusion post-MI. The findings presented here demonstrate that EC-specific reduction in mito-ROS using overexpresion of mitochondrial antioxidant MnSOD, induced mitochondrial complex I biogenesis, increased OXPHOS in coronary EC,

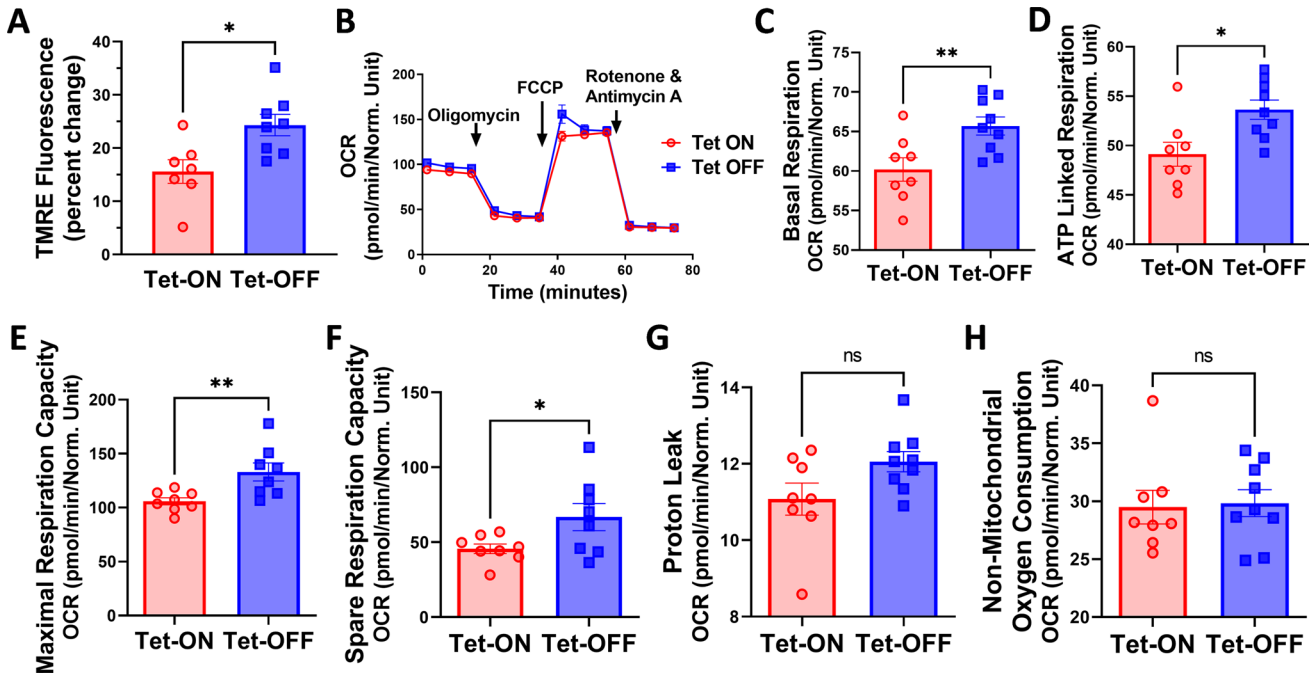

Fig. 9 MnSOD-OE increases mitochondrial membrane potential and improves mitochondrial respiration in MHEC. **A** Quantitative analysis of mitochondrial membrane potential estimated by TMRE fluorescence in a plate reader. **B** Seahorse experiment showing oxygen consumption rate (OCR) after treatment with Oligomycin, FCCP, or Rotenone and Antimycin A. A quantitative analysis of OCR measurement by seahorse showed a significant increase in **C** calculated basal respiration, **D** ATP linked respiration, **E** maximal and **F** spare respiration capacity. There were no changes in **G** proton leak and **H** non-mitochondrial O_2 consumption. All experiments were performed in triplicate using three independent preparations of MHEC (each isolated using 2–4 animal hearts/group). $n = 7$–8 wells/group (**A**); $n = 8$–9 wells/group (**B** and **C**). $^*p < 0.05$; $^{**}p < 0.01$

and induced coronary angiogenesis in ischemic myocardium in a post-MI (permanent LAD ligation) model resulting in significant recovery of cardiac function after non-reperfused MI (Fig. 11). Although recent advancements in the management of CVD have improved longevity globally, CVD remains the number one cause of mortality [64]. Invasive treatments including stenting and coronary artery bypass graft (CABG) surgeries appear to be the treatment of choice in acute and chronic myocardial ischemia associated with coronary artery disease. Together, these emphasize the need for the development of innovative non-invasive treatment modalities that will help improve coronary vascular health. To that end, one specific approach can be to devise a mechanism that will render coronary vascular endothelium resilient during acute MI and/or chronic myocardial ischemia. This may, in turn, help improve retention of existing coronary vessels and/or induce coronary angiogenesis in ischemic myocardium, and thus help prevent myocardial remodeling and loss of cardiac function.

The relationship between ROS and EC survival and proliferation has emerged as an area of particular interest. Experimental models of acute MI, chronic ischemia, and ischemia/reperfusion have shown increased oxidative stress that results in endothelial dysfunction [69], EC death [52], reduction in coronary vascular density [45], cardiac remodeling [21], and eventual heart failure [14]. Paradoxically, however, clinical trials with global antioxidant treatments were ineffective, or even deleterious, in CVD treatment [11, 12]. While these findings demonstrated the limitation of global antioxidant treatments, they have inspired studies into subcellular ROS modulation. We have recently reported paradoxical improvement and detrimental signaling, angiogenesis, and endothelial function with short-term versus long-term endothelium-specific NOX2 OE, respectively, in a transgenic animal model, highlighting the importance of EC mito-ROS homeostasis [49, 50]. Since the finding that a short-term increase in NOX2-derived ROS results in the upregulation of MnSOD and angiogenesis, several studies have reported beneficial effects of MnSOD-mimetics on cardiac recovery and angiogenesis [15, 19, 66]. However, the mito-ROS scavenging agents used in those studies were not EC-specific and thus might have modulated mito-ROS of different cell types including cardiomyocytes, vascular smooth muscle cells, and fibroblasts. Due to the absence of specificity of SOD mimetics, it is unknown whether coronary angiogenesis and cardiac funcion recovery are solely a result of EC ROS regulation or if other cells could play a role in functional recovery. Interestingly, cardiac muscle-specific

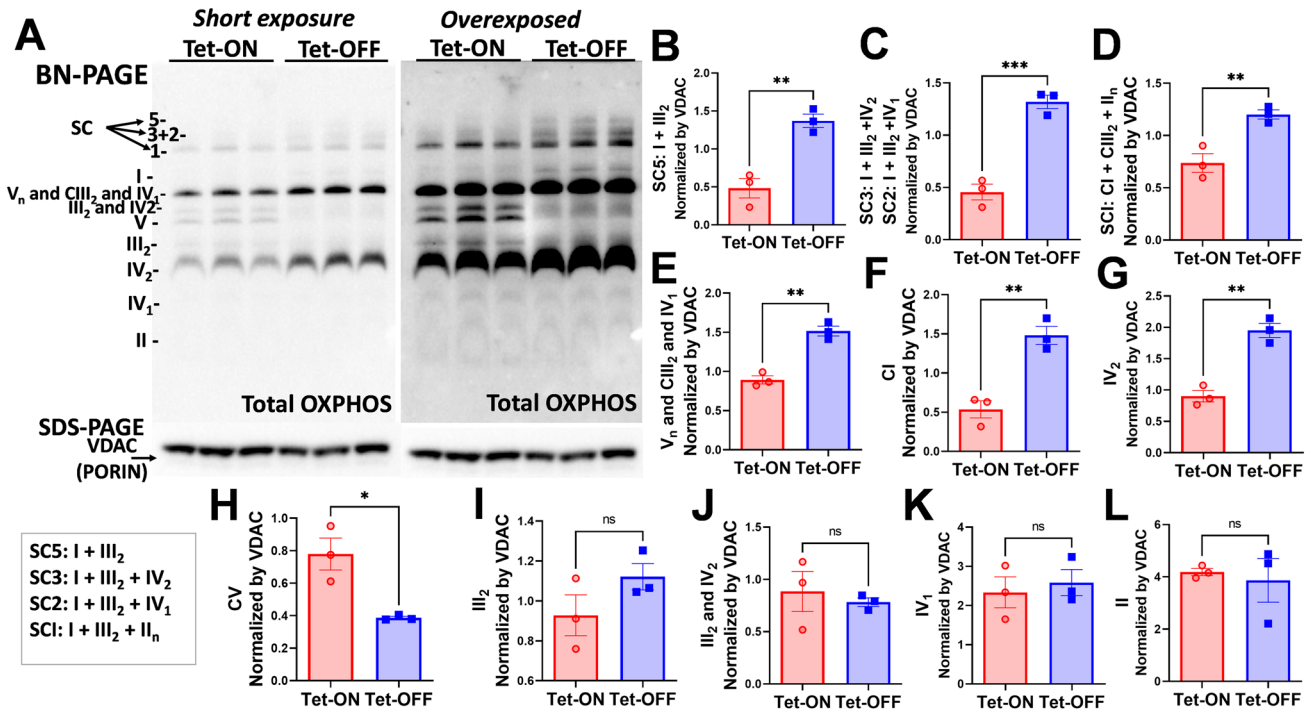

Fig. 10 Reduced mito-ROS increases the organizational assembly of mitochondrial complexes into supercomplexes in EC. **A** Native-PAGE western blot image showing the organization of mitochondrial complexes and supercomplexes in control (Tet-ON) versus MnSOD-OE (Tet-OFF) MHEC. **B** Quantitative analysis of SC5. **C** Quantitative analysis of SC3 and SC2. **D** Quantitative analysis of SC1. **E** Quantitative analysis of SC formed by $CV_n + CIII_2 + IV_1$. **F** Quantitative analysis of free CI. **G** Quantitative analysis of CIV_2. **H** Quantitative analysis of SC formed by CV. **I** Quantitative analysis of $CIII_2$. **J** Quantitative analysis of $CIII_2 + CIV_2$. **K** Quantitative analysis of SC formed by CIV_1. **L** Quantitative analysis of CII. Statistical analysis was carried out by two-tailed unpaired Student's *t* test. $n = 3$/group (each sample represents an independent preparation of MHEC isolated using 3 animal hearts/group). $^*p < 0.05$; $^{**}p < 0.01$; $^{***}p < 0.001$. *Tet-ON* MnSOD Control, *Tet-OFF* MnSOD-OE, *SC* supercomplex

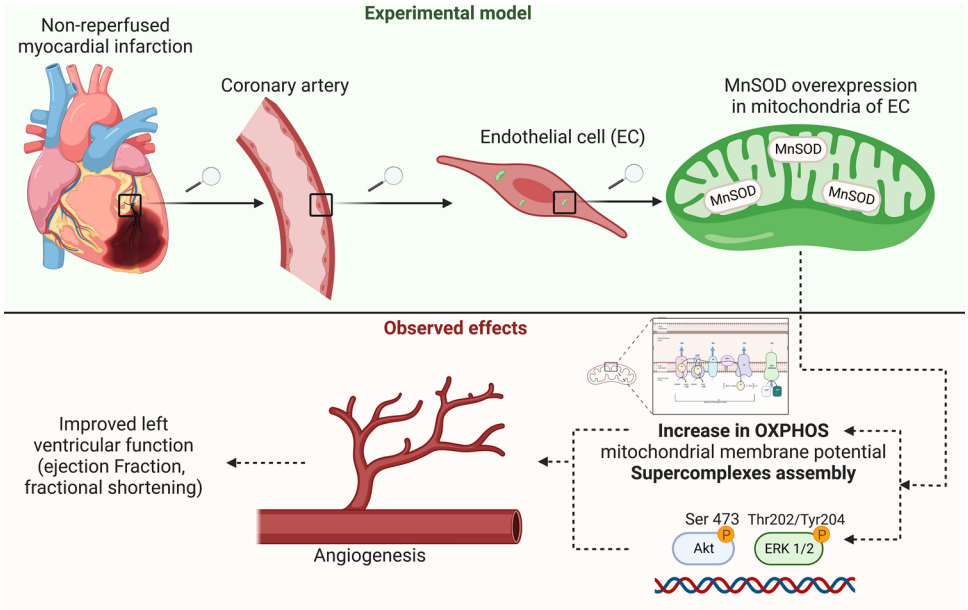

Fig. 11 Summary of findings and suggested hypothesis. MnSOD OE increases OXPHOS, membrane potential, and the assembly of supercomplexes in mitochondria of mouse heart ECs. These effects are associated with angiogenesis and improvement in cardiac function in a non-reperfused MI

overexpression of MnSOD was shown to reduce infarction area in a non-survival model of ischemia–reperfusion injury, however, its effect on coronary vessel density and function were not investigated [4].

The present study demonstrates that an endothelium-specific and mitochondria-localized decrease in ROS can result in subcellular changes in EC resulting in improvement in coronary angiogenesis. It is shown here, for the first time, that transgenic OE of MnSOD specifically in ECs provides reduced levels of mito-ROS as confirmed by the Mito-roGFP assay in MnSOD-OE MHEC. This reduced mito-ROS in EC were accompanied by increased coronary vascular density and a significant reduction in the size of myocardial infarct in the non-reperfused MI model. Echocardiography showed that ischemic myocardium with decreased mito-ROS in coronary vascular endothelium had significant improvement in their left ventricular EF and FS in non-reperfused post-MI hearts. Together, these findings suggest that MnSOD-OE animals with reduced mito-ROS in EC have significant improvement in the non-reperfused post-MI recovery of cardiac function due to coronary angiogenesis.

Increased proliferation of EC and formation of new capillaries in ischemic myocardium observed in this study suggest that EC-specific reduction in mito-ROS renders EC resilient during myocardial ischemia. Although we have yet to elucidate the precise molecular mechanisms, previous studies have reported hydrogen peroxide, a product of MnSOD activity, as an inducer of angiogenesis. Yasuda and collaborators have previously shown that hydrogen peroxide stimulates angiogenesis by inducing EC proliferation and migration, which was associated with increased mRNA levels of one of the erythroblast transformation-specific (ETS) transcription factors [67]. Shijun et al. reported that hydrogen peroxide promoted cell migration by activation of ERK 1/2 [38]. Indeed, MnSOD-OE showed ERK 1/2 activation and increased EC migration in our study. Similarly, PI3K/Akt pathway was found to be activated in our study, which has been recently shown to contribute to the activation of the ETS-related gene (ERG), an ETS transcription factor involved in the control of notch signaling, angiogenesis and vascular stabilization [51]. Other studies have shown that activation of the ROS/Akt/ERK signaling was associated with post-MI cardioprotection in rats [70].

EC is known to derive most of its ATP (> 85%) via glycolysis [18]. Interestingly, one of the most striking findings in our study is that ECs in MnSOD-OE animals demontrated a significant increase in their mitochondrial OXPHOS as measured by increased OCR using seahose. It is worthwhile to mention that in EC normally less than 15% of ATP synthesis occurs in mitochondria, while the majority of EC's energy comes from less-efficiant anerobic glycolysis. It is not known why ECs, like tumor cells, prefer glycolysis that produces two ATP from one module of glucose to a much more energy-eficient system OXPHOS that synthesizes 32 to 34 ATP moleculae from one molecule of glucose. It is plausible that a reduction in mito-ROS, which results in increased mitochondrial membrane potential and is associated with increased involvement of OXPHOS for energy production may help cope ECs in ischemic myocardium (post-MI), where nutrition (glucose) is likely to be scarce. It is plausible that the observed coronary angiogenesis in non-reperfused ischemic myocardum is fueled by this improvement in energy generation in MnSOD-OE ECs. This notion derives its support from our observation that MnSOD-OE ECs also have increased expression of mitochondrial complexes I and IV, as well as an increase in mitochondrial membrane potential and supercomplexes assembly. Corroborating with our data, antioxidants and MnSOD mimetics have been shown to enhance OXPHOS, mitochondrial membrane potential and mitochondrial supercomplex formation in other cell (non-EC) types such as fibroblasts, cardiomyocytes, and in the piriform cortex [9, 33, 54]. It has recently been reported that human EC containing telomerase reverse transcriptase in mitochondria, which results in a decrease in mito-ROS, induces an increase in migration potential, activation of eNOS, and enhanced Complex I activity in EC [7]. Another study proposed an increase in mitochondrial OXPHOS may result in improved energy supply to the cell as a desired aspect of a potential treatment for heart failure [13]. In addition, as described by Kiyooka and collaborators, the integrity of mitochondrial DNA and the function of mitochondrial complex machinery are critical for endothelium-dependent vasodilation in CVD [31]. In fact, treatment with the non-specific mito-ROS scavenger Mito-Tempo was shown to enhance coronary relaxation in diabetes and non-diabetes setting in an ex vivo cardioplegic hypoxia-reoxygenation model [53]. Further studies will be required to determine the molecular mechanisms by which reduced mito-ROS induce biogenesis of mitochondrial complexes, enhancement of supercomplexes formation, alter the energy generation balance between anerobic glycolysis and oxidative phosphorylation, and whether this metabolic reprogramming in EC plays a direct role in coronary angiogenesis in ischemic myocardium.

In conclusion, the fact that coronary angiogenesis and improvement in cardiac function were achieved by a reduction in mito-ROS in an EC-specific manner is intriguing. Our data suggest that EC mitochondria may play an essential role in cardiovascular homeostasis more than previously thought.

As a future directive, it will be important to determine whether PI3K and/or ERK1/2 is activated via an H_2O_2-dependent signaling cascade in MnSOD-OE EC; a question that we plan to address in a future study using transgenic animals with or without an increase in catalase. It would also be important to determine whether Akt and

ERK1/2 activation directly mediate angiogenesis and the improvement of cardiac function in this model, which could be evaluated by chemically blocking Akt and ERK activation. Another future perspective would be to test mito-ROS scavengers XJB-5–131 [19, 28] and JP4-039 [22, 33] in MI model. The latter is already under preliminary investigation in our laboratory. Finally, the development and investigation of EC-targeted specific mito-ROS scavengers could aid our understanding about EC mitochondria's role in the recovery of cardiac function in myocardial ischemia.

This study also raises several interesting questions that need to be addressed in the future: (1) how does MnSOD-OE in EC mitochondria results in increased OXPHOS, for instance, what specific signaling modulation and/or anabolic changes in the citric acid cycle are contributing to OXPHOS; (2) what are the relative contribution of OXPHOS versus glycolysis to energy generation in MnSOD-OE ECs; (3) does increase in OXPHOS induce a metabolic shift in ECs which in turn provides resilience and survival benefits to EC during ischemia; (4) is increased OXPHOS a result of improvement in mitochondrial supercomplex formation and ETC; and (5) where do EC mitochondria derive oxygen for oxidative phosphorylation during ischemic insult in the myocardium. Ongoing studies in our lab will address these critical queries.

Study limitations

A limitation of this study is that the MI model of permanent occlusion of the coronary artery does not represent most MI patients that currently receive reperfusion therapy. For these patients, the model of ischemia–reperfusion would be more adequate. Nevertheless, the permanent ligation model that we have used in this study can provide valuable information for those 15–25% patients (globally 3 million people) that do not receive reperfusion in a timely manner [36]. Another limitation is the absence of comorbidities in our model. For example, a model of vascular disease associated with MI would provide more translational findings, as a vascular disease is an underlying factor of CVD. We plan to address the above issues in future studies.

Supplementary Information The online version contains supplementary material available at https://doi.org/10.1007/s00395-022-00976-x.

Acknowledgements We would like to thank Dr. Gideon Koren and Dr. Olin Liang for their kind access to the ultrasound system and imaging microscopes. We acknowledge the COBRE Center for Cancer Research Development, Proteomics Core Facility, Rhode Island Hospital, Providence, RI, for their help with proteomic sample processing and LC-MS/MS analysis. We would also like to thank Penny Cloutier-Lyons and veterinary medical staff for veterinary support, and Dr. Guangbin Shi, Dr. Karla Braga, and Lelia Noble for technical support. Figure 11 was produced using Biorender.

Author contributions RBT: data collection and analysis, manuscript preparation and critical review. MP: data collection and analysis, critical review of the manuscript. PZ: data collection and analysis, critical review of the manuscript. ES: data collection and analysis, final review of the manuscript. BC: data collection and analysis, final review of the manuscript. CK: manuscript preparation and critical review. NA: data collection and analysis, critical review of the manuscript. FWS: critical review of the manuscript. MRA: study conceptualization and design, data interpretation, manuscript edits, critical review, and submission.

Funding This work was supported by NIH/NHLBI/NIGMS 1R01 HL133624-01A1 and 2R56 HL133624-05 (MRA). PZ was supported by NIGMS/NIH 5P20GM103652.

Availability of data and material All supporting data are available within the article and its online supplementary files. Raw data from this study are available from the corresponding author upon reasonable request.

Code availability Not applicable.

Declarations

Conflict of interest On behalf of all authors, the corresponding author states that there is no conflict of interest or competing interests. M.R.A. is the co-founder of a non-profit organization Health and Education for All (HAEFA) USA and has served as a consultant for ARI Science, MA, USA for COVID-19 studies.

Ethics approval This study was carried out under the approved protocol number 0093-16 of the Lifespan Institutional Animal Care and Use Committee of the Rhode Island Hospital. All the ethical regulations were strictly followed as established by the Animal Welfare Act, the Public Health Service Policy on Humane Care and Use of Laboratory Animals, the Guide for the Care and Use of Laboratory Animals, and the ethical standards laid down by the 1964 Declaration of Helsinki and its later amendments.

Consent to participate The manuscript does not contain clinical studies or patient data.

References

1. Abid MR, Kachra Z, Spokes KC, Aird WC (2000) NADPH oxidase activity is required for endothelial cell proliferation and migration. FEBS Lett 486:252–256. https://doi.org/10.1016/S0014-5793(00)02305-X
2. Abid MR, Spokes KC, Shih SC, Aird WC (2007) NADPH oxidase activity selectively modulates vascular endothelial growth factor signaling pathways. J Biol Chem 282:35373–35385. https://doi.org/10.1074/jbc.M702175200
3. Abid MR, Tsai JC, Spokes KC, Deshpande SS, Irani K, Aird WC (2001) Vascular endothelial growth factor induces manganese-superoxide dismutase expression in endothelial cells by a Rac1-regulated NADPH oxidase-dependent mechanism. FASEB J 15:2548–2550. https://doi.org/10.1096/fj.01-0338fje
4. Abunasra HJ, Smolenski RT, Morrison K, Yap J, Sheppard MN, O'brien T, Suzuki K, Jayakumar J, Yacoub MH, (2001) Efficacy of adenoviral gene transfer with manganese superoxide dismutase and endothelial nitric oxide synthase in reducing ischemia and reperfusion injury. Eur J Cardio Thorac Surg 20:153–158. https://doi.org/10.1016/s1010-7940(01)00704-7

5. Ahsan N, Belmont J, Chen Z, Clifton JG, Salomon AR (2017) Highly reproducible improved label-free quantitative analysis of cellular phosphoproteome by optimization of LC-MS/MS gradient and analytical column construction. J Proteom. https://doi.org/10.1016/j.jprot.2017.06.013
6. Aldosari S, Awad M, Harrington EO, Sellke FW, Ruhul Abid M (2018) Subcellular reactive oxygen species (ROS) in cardiovascular pathophysiology. Antioxidants. https://doi.org/10.3390/antiox7010014
7. Ale-Agha N, Jakobs P, Goy C, Zurek M, Rosen J, Dyballa-Rukes N, Metzger S, Greulich J, von Ameln F, Eckermann O, Unfried K, Brack F, Grandoch M, Thielmann M, Kamler M, Gedik N, Kleinbongard P, Heinen A, Heusch G, Gödecke A, Altschmied J, Haendeler J (2021) Mitochondrial telomerase reverse transcriptase protects from myocardial ischemia/reperfusion injury by improving complex I composition and function. Circulation 144:1876–1890. https://doi.org/10.1161/CIRCULATIONAHA.120.051923
8. Alhayaza R, Haque E, Karbasiafshar C, Sellke FW, Abid MR (2020) The relationship between reactive oxygen species and endothelial cell metabolism. Front Chem. https://doi.org/10.3389/FCHEM.2020.592688
9. Anwar MR, Saldana-Caboverde A, Garcia S, Diaz F (2018) The organization of mitochondrial supercomplexes is modulated by oxidative stress in vivo in mouse models of mitochondrial encephalopathy. Int J Mol Sci. https://doi.org/10.3390/IJMS19061582
10. Benjamin EJ, Paul Muntner C, Alvaro Alonso V, Marcio Bittencourt FS, Clifton Callaway MW, April Carson FP, Alanna Chamberlain FM, Chang AR, Susan Cheng M, Sandeep Das FR, Francesca Delling FN, Luc Djousse M, Mitchell Elkind MS, Jane Ferguson FF, Myriam Fornage F, WRITING GROUP MEMBERS On behalf of the American Heart Association Council on Epidemiology and Prevention Statistics Committee and Stroke Statistics Subcommittee (2019) Heart disease and stroke statistics—2019 update: a report from the American Heart Association. Circulation 139:e56–e528. https://doi.org/10.1161/CIR.0000000000000659
11. Bjelakovic G, Nikolova D, Gluud C (2013) Meta-regression analyses, meta-analyses, and trial sequential analyses of the effects of supplementation with beta-carotene, vitamin A, and vitamin E singly or in different combinations on all-cause mortality: do we have evidence for lack of harm? PLoS One. https://doi.org/10.1371/journal.pone.0074558
12. Bjelakovic G, Nikolova D, Gluud LL, Simonetti RG, Gluud C (2007) Mortality in randomized trials of antioxidant supplements for primary and secondary prevention: systematic review and meta-analysis. J Am Med Assoc 297:842–857. https://doi.org/10.1001/jama.297.8.842
13. Brown DA, Perry JB, Allen ME, Sabbah HN, Stauffer BL, Shaikh SR, Cleland JGF, Colucci WS, Butler J, Voors AA, Anker SD, Pitt B, Pieske B, Filippatos G, Greene SJ, Gheorghiade M (2017) Expert consensus document: mitochondrial function as a therapeutic target in heart failure. Nat Rev Cardiol 14:238–250. https://doi.org/10.1038/nrcardio.2016.203
14. Chen Y-RR, Zweier JL (2014) Cardiac mitochondria and reactive oxygen species generation. Circ Res 114:524–537. https://doi.org/10.1161/CIRCRESAHA.114.300559
15. Cheng Y, Liu DZ, Zhang CX, Cui H, Liu M, Zhang BL, Mei QB, Lu ZF, Zhou SY (2019) Mitochondria-targeted antioxidant delivery for precise treatment of myocardial ischemia-reperfusion injury through a multistage continuous targeted strategy. Nanomed Nanotechnol Biol Med 16:236–249. https://doi.org/10.1016/J.NANO.2018.12.014
16. Cormier N, Yeo A, Fiorentino E, Paxson J (2015) Optimization of the wound scratch assay to detect changes in murine mesenchymal stromal cell migration after damage by soluble cigarette smoke extract. J Vis Exp. https://doi.org/10.3791/53414
17. Davidson SM (2010) Endothelial mitochondria and heart disease. Cardiovasc Res 88:58–66. https://doi.org/10.1093/cvr/cvq195
18. De-Bock K, Georgiadou M, Schoors S, Kuchnio A, Wong BW, Cantelmo AR, Quaegebeur A, Ghesquière B, Cauwenberghs S, Eelen G, Phng L-KK, Betz I, Tembuyser B, Brepoels K, Welti J, Geudens I, Segura I, Cruys B, Bifari F, Decimo I, Blanco R, Wyns S, Vangindertael J, Rocha S, Collins RT, Munck S, Daelemans D, Imamura H, Devlieger R, Rider M, Van Veldhoven PP, Schuit F, Bartrons R, Hofkens J, Fraisl P, Telang S, Deberardinis RJ, Schoonjans L, Vinckier S, Chesney J, Gerhardt H, Dewerchin M, Carmeliet P, Ghesquiè B, Cauwenberghs S, Eelen G, Phng L-KK, Betz I, Tembuyser B, Brepoels K, Welti J, Geudens I, Segura I, Cruys B, Bifari F, Decimo I, Blanco R, Wyns S, Vangindertael J, Rocha S, Collins RT, Munck S, Daelemans D, Imamura H, Devlieger R, Rider M, Van Veldhoven PP, Schuit F, Bartrons R, Hofkens J, Fraisl P, Telang S, Deberardinis RJ, Schoonjans L, Vinckier S, Chesney J, Gerhardt H, Dewerchin M, Carmeliet P (2013) Role of PFKFB3-driven glycolysis in vessel sprouting. Cell 154:651–663. https://doi.org/10.1016/j.cell.2013.06.037
19. Escobales N, Nuñez RE, Jang S, Parodi-Rullan R, Ayala-Peña S, Sacher JR, Skoda EM, Wipf P, Frontera W, Javadov S (2014) Mitochondria-targeted ROS scavenger improves post-ischemic recovery of cardiac function and attenuates mitochondrial abnormalities in aged rats. J Mol Cell Cardiol 77:136–146. https://doi.org/10.1016/j.yjmcc.2014.10.009
20. Fan LM, Douglas G, Bendall JK, McNeill E, Crabtree MJ, Hale AB, Li JM, McAteer MA, Schneider JE, Choudhury RP, Channon KM (2014) Endothelial cell-specific reactive oxygen species production increases susceptibility to aortic dissection. Circulation 129:2661–2672. https://doi.org/10.1161/CIRCULATIONAHA.113.005062
21. Guo X, Yan F, Li J, Zhang C, Su H, Bu P (2020) SIRT3 ablation deteriorates obesity-related cardiac remodeling by modulating ROS-NF-κB-MCP-1 signaling pathway. J Cardiovasc Pharmacol 76:296–304. https://doi.org/10.1097/FJC.0000000000000877
22. Hamedani Y, Teixeira RB, Karbasiafshar C, Wipf P, Bhowmick S, Abid MR (2021) Delivery of a mitochondria-targeted antioxidant from biocompatible, polymeric nanofibrous scaffolds. FEBS Open Bio 11:35–47. https://doi.org/10.1002/2211-5463.13032
23. Harrison D, Griendling KK, Landmesser U, Hornig B, Drexler H (2003) Role of oxidative stress in atherosclerosis. Am J Cardiol 91:7A–11A. https://doi.org/10.1016/s0002-9149(02)03144-2
24. Hausenloy DJ, Chilian W, Crea F, Davidson SM, Ferdinandy P, Garcia-Dorado D, Van Royen N, Schulz R, Heusch G (2019) The coronary circulation in acute myocardial ischaemia/reperfusion injury: a target for cardioprotection. Cardiovasc Res 115:1143–1155. https://doi.org/10.1093/CVR/CVY286
25. Heusch G (2016) The coronary circulation as a target of cardioprotection. Circ Res 118:1643–1658. https://doi.org/10.1161/CIRCRESAHA.116.308640
26. Heusch G (2019) Coronary microvascular obstruction: the new frontier in cardioprotection. Basic Res Cardiol 114:45. https://doi.org/10.1007/s00395-019-0756-8
27. Irani K (2000) Oxidant signaling in vascular cell growth, death, and survival. Circ Res 87:179–183. https://doi.org/10.1161/01.RES.87.3.179
28. Javadov S, Jang S, Rodriguez-Reyes N, Rodriguez-Zayas AE, Soto Hernandez J, Krainz T, Wipf P, Frontera W (2015) Mitochondria-targeted antioxidant preserves contractile properties and mitochondrial function of skeletal muscle in aged rats. Oncotarget 6:39469–39481. https://doi.org/10.18632/oncotarget.5783
29. Jha P, Wang X, Auwerx J (2016) Analysis of mitochondrial respiratory chain supercomplexes using blue native polyacrylamide gel electrophoresis (BN-PAGE). Curr Protoc Mouse Biol 6:1. https://doi.org/10.1002/9780470942390.MO150182

30. Johns TNP, Olson BJ (1954) Experimental myocardial infarction. I. A method of coronary occlusion in small animals. Ann Surg 140:675–682. https://doi.org/10.1097/00000658-195411000-00006
31. Kiyooka T, Ohanyan V, Yin L, Pung YF, Chen YR, Chen CL, Kang PT, Hardwick JP, Yun J, Janota D, Peng J, Kolz C, Guarini G, Wilson G, Shokolenko I, Stevens DA, Chilian WM (2022) Mitochondrial DNA integrity and function are critical for endothelium-dependent vasodilation in rats with metabolic syndrome. Basic Res Cardiol 1171(117):1–15. https://doi.org/10.1007/S00395-021-00908-1
32. Lebovitz RM, Zhang H, Vogel H, Cartwright J, Dionne L, Lu N, Huang S, Matzuk MM (1996) Neurodegeneration, myocardial injury, and perinatal death in mitochondrial superoxide dismutase-deficient mice. Proc Natl Acad Sci USA 93:9782–9787. https://doi.org/10.1073/pnas.93.18.9782
33. Leipnitz G, Mohsen AW, Karunanidhi A, Seminotti B, Roginskaya VY, Markantone DM, Grings M, Mihalik SJ, Wipf P, Van Houten B, Vockley J (2018) Evaluation of mitochondrial bioenergetics, dynamics, endoplasmic reticulum-mitochondria cross-talk, and reactive oxygen species in fibroblasts from patients with complex I deficiency. Sci Rep 8:1–14. https://doi.org/10.1038/s41598-018-19543-3
34. Li J, Zhao Y, Zhu W (2022) Targeting angiogenesis in myocardial infarction: novel therapeutics (review). Exp Ther Med. https://doi.org/10.3892/ETM.2021.10986
35. Li Y, Huang TT, Carlson EJ, Melov S, Ursell PC, Olson JL, Noble LJ, Yoshimura MP, Berger C, Chan PH, Wallace DC, Epstein CJ (1995) Dilated cardiomyopathy and neonatal lethality in mutant mice lacking manganese superoxide dismutase. Nat Genet 11:376–381. https://doi.org/10.1038/ng1295-376
36. Lindsey ML, Bolli R, Canty JM, Du X-J, Frangogiannis NG, Frantz S, Gourdie RG, Holmes JW, Jones SP, Kloner RA, Lefer DJ, Liao R, Murphy E, Ping P, Przyklenk K, Recchia FA, Schwartz Longacre L, Ripplinger CM, Van Eyk JE, Heusch G (2018) Guidelines for experimental models of myocardial ischemia and infarction. Am J Physiol Circ Physiol 314:H812–H838. https://doi.org/10.1152/ajpheart.00335.2017
37. Lu Q, Mundy M, Chambers E, Lange T, Newton J, Borgas D, Yao H, Choudhary G, Basak R, Oldham M, Rounds S (2017) Alda-1 protects against acrolein-induced acute lung injury and endothelial barrier dysfunction. Am J Respir Cell Mol Biol 57:662–673. https://doi.org/10.1165/rcmb.2016-0342OC
38. Ma S, Fu A, Lim S, Chiew GGY, Luo KQ (2018) MnSOD mediates shear stress-promoted tumor cell migration and adhesion. Free Radic Biol Med 129:46–58. https://doi.org/10.1016/j.freeradbiomed.2018.09.004
39. Masson P (1929) Trichrome stainings and their preliminary techniques. J Tech Met 12:75
40. Muntean DM, Sturza A, Dănilă MD, Borza C, Duicu OM, Mornoș C (2016) The role of mitochondrial reactive oxygen species in cardiovascular injury and protective strategies. Oxid Med Cell Longev 2016:1–19. https://doi.org/10.1155/2016/8254942
41. Niccoli G, Montone RA, Ibanez B, Thiele H, Crea F, Heusch G, Bulluck H, Hausenloy DJ, Berry C, Stiermaier T, Camici PG, Eitel I (2019) Optimized treatment of ST-elevation myocardial infarction. Circ Res 125:245–258. https://doi.org/10.1161/CIRCRESAHA.119.315344
42. Nozawa E, Kanashiro RM, Murad N, Carvalho ACC, Cravo SLD, Campos O, Tucci PJF, Moises VA (2006) Performance of two-dimensional Doppler echocardiography for the assessment of infarct size and left ventricular function in rats. Braz J Med Biol Res Rev Bras Pesqui medicas e Biol 39:687–695. https://doi.org/10.1590/S0100-879X2006000500016
43. Paiva SAR, Matsubara LS, Matsubara BB, Minicucci MF, Azevedo PS, Campana ÁO, Zornoff LAM (2005) Retinoic acid supplementation attenuates ventricular remodeling after myocardial infarction in rats. J Nutr 135:2326–2328. https://doi.org/10.1093/JN/135.10.2326
44. Pinto AR, Ilinykh A, Ivey MJ, Kuwabara JT, D'Antoni ML, Debuque R, Chandran A, Wang L, Arora K, Rosenthal NA, Tallquist MD, D'antoni ML, Debuque R, Chandran A, Wang L, Arora K, Rosenthal NA, Tallquist MD (2016) Revisiting cardiac cellular composition. Circ Res 118:400–409. https://doi.org/10.1161/CIRCRESAHA.115.307778
45. Prech M, Grajek S, Marszalek A, Lesiak M, Jemielity M, Araszkiewicz A, Mularek-Kubzdela T, Cieslinski A (2006) Chronic infarct-related artery occlusion is associated with a reduction in capillary density. Effects on infarct healing. Eur J Heart Fail 8:373–380. https://doi.org/10.1016/J.EJHEART.2005.10.016
46. Reichert K, Colantuono B, McCormack I, Rodrigues F, Pavlov V, Abid MR (2017) Murine left anterior descending (LAD) coronary artery ligation: an improved and simplified model for myocardial infarction. J Vis Exp. https://doi.org/10.3791/55353
47. San Martin A, Griendling KK (2014) NADPH oxidases: progress and opportunities. Antioxid Redox Signal 20:2692–2694. https://doi.org/10.1089/ars.2014.5947
48. Scrimgeour LA, Potz BA, AboulGheit A, Shi G, Stanley M, Zhang Z, Sodha NR, Ahsan N, Abid MR, Sellke FW (2019) Extracellular vesicles promote arteriogenesis in chronically ischemic myocardium in the setting of metabolic syndrome. J Am Heart Assoc. https://doi.org/10.1161/JAHA.119.012617
49. Shafique E, Choy WC, Liu Y, Feng J, Cordeiro B, Lyra A, Arafah M, Yassin-Kassab A, Zanetti AVD, Clements RT, Bianchi C, Benjamin LE, Sellke FW, Abid MR (2013) Oxidative stress improves coronary endothelial function through activation of the pro-survival kinase AMPK. Aging (Albany NY) 5:515–530. https://doi.org/10.18632/aging.100569
50. Shafique E, Torina A, Reichert K, Colantuono B, Nur N, Zeeshan K, Ravichandran V, Liu Y, Feng J, Zeeshan K, Benjamin LE, Irani K, Harrington EO, Sellke FW, Abid MR, Ruhul Abid M, Abid MR (2017) Mitochondrial redox plays a critical role in the paradoxical effects of NAPDH oxidase-derived ROS on coronary endothelium. Cardiovasc Res 113:234–246. https://doi.org/10.1093/cvr/cvw249
51. Shah AV, Birdsey GM, Peghaire C, Pitulescu ME, Dufton NP, Yang Y, Weinberg I, Osuna Almagro L, Payne L, Mason JC, Gerhardt H, Adams RH, Randi AM (2017) The endothelial transcription factor ERG mediates angiopoietin-1-dependent control of Notch signalling and vascular stability. Nat Commun. https://doi.org/10.1038/ncomms16002
52. Shi H, Gao Y, Dong Z, Yang J, Gao R, Li X, Zhang S, Ma L, Sun X, Wang Z, Zhang F, Hu K, Sun A, Ge J (2021) GSDMD-mediated cardiomyocyte pyroptosis promotes myocardial I/R injury. Circ Res 129:383–396. https://doi.org/10.1161/CIRCRESAHA.120.318629
53. Song Y, Xing H, He Y, Zhang Z, Shi G, Wu S, Liu Y, Harrington EO, Sellke FW, Feng J (2021) Inhibition of mitochondrial reactive oxygen species improves coronary endothelial function after cardioplegic hypoxia/reoxygenation. J Thorac Cardiovasc Surg. https://doi.org/10.1016/J.JTCVS.2021.06.029
54. Sudheesh NP, Ajith TA, Janardhanan KK (2013) Ganoderma lucidum ameliorate mitochondrial damage in isoproterenol-induced myocardial infarction in rats by enhancing the activities of TCA cycle enzymes and respiratory chain complexes. Int J Cardiol 165:117–125. https://doi.org/10.1016/j.ijcard.2011.07.103
55. Takagawa J, Zhang Y, Wong ML, Sievers RE, Kapasi NK, Wang Y, Yeghiazarians Y, Lee RJ, Grossman W, Springer ML (2007) Myocardial infarct size measurement in the mouse chronic infarction model: comparison of area- and length-based approaches. J Appl Physiol 102:2104–2111. https://doi.org/10.1152/japplphysiol.00033.2007

56. Teixeira RB, Karbasiafshar C, Sabra M, Abid MR (2021) Optimization of mito-roGFP protocol to measure mitochondrial oxidative status in human coronary artery endothelial cells. STAR Protoc 2:100753. https://doi.org/10.1016/j.xpro.2021.100753
57. Teixeira RB, Zimmer A, de Castro AL, de Lima-Seolin BG, Türck P, Siqueira R, Belló-Klein A, Singal PK, da Rosa Araujo AS (2017) Long-term T3 and T4 treatment as an alternative to aerobic exercise training in improving cardiac function post-myocardial infarction. Biomed Pharmacother 95:965–973. https://doi.org/10.1016/j.biopha.2017.09.021
58. Tombor LS, Dimmeler S (2022) Why is endothelial resilience key to maintain cardiac health? Basic Res Cardiol 117:35. https://doi.org/10.1007/S00395-022-00941-8
59. Truett GE, Heeger P, Mynatt RL, Truett AA, Walker JA, Warman ML (2000) Preparation of PCR-quality mouse genomic DNA with hot sodium hydroxide and Tris (HotSHOT). Biotech 29:52–54. https://doi.org/10.2144/00291bm09
60. Van-der-Laan AM, Piek JJ, van Royen N (2009) Targeting angiogenesis to restore the microcirculation after reperfused MI. Nat Rev Cardiol 68(6):515–523. https://doi.org/10.1038/nrcardio.2009.103
61. Wannamethee SG, Bruckdorfer KR, Shaper AG, Papacosta O, Lennon L, Whincup PH (2013) Plasma vitamin C, but not vitamin E, is associated with reduced risk of heart failure in older men. Circ Heart Fail 6:647–654. https://doi.org/10.1161/CIRCHEARTFAILURE.112.000281
62. Wilhelm K, Happel K, Eelen G, Schoors S, Oellerich MF, Lim R, Zimmermann B, Aspalter IM, Franco CA, Boettger T, Braun T, Fruttiger M, Rajewsky K, Keller C, Brüning JC, Gerhardt H, Carmeliet P, Potente M (2016) FOXO1 couples metabolic activity and growth state in the vascular endothelium. Nature 529:216–220. https://doi.org/10.1038/NATURE16498
63. World Health Organization (2018) Global health estimates 2016: disease burden by cause, age, sex, by country and by region, 2000–2016. https://www.who.int/healthinfo/global_burden_disease/estimates/en/index1.html. Accessed 2 Mar 2022
64. World Health Organization (2020) The top 10 causes of death. https://www.who.int/news-room/fact-sheets/detail/the-top-10-causes-of-death. Accessed 2 Mar 2022
65. Wu M, Huang Z, Zeng L, Wang C, Wang D (2022) Programmed cell death of endothelial cells in myocardial infarction and its potential therapeutic strategy. Cardiol Res Pract 2022:1–10. https://doi.org/10.1155/2022/6558060
66. Xiao Y, Yim K, Zhang H, Bakker D, Nederlof R, Smeitink JAM, Renkema H, Hollmann MW, Weber NC, Zuurbier CJ (2021) the redox modulating sonlicromanol active metabolite KH176m and the antioxidant mpg protect against short-duration cardiac ischemia-reperfusion injury. Cardiovasc Drugs Ther 35:745–758. https://doi.org/10.1007/s10557-021-07189-9
67. Yasuda M, Ohzeki Y, Shimizu S, Naito S, Ohtsuru A, Yamamoto T, Kuroiwa Y (1998) Stimulation of in vitro angiogenesis by hydrogen peroxide and the relation with ets-1 in endothelial cells. Life Sci 64:249–258. https://doi.org/10.1016/S0024-3205(98)00560-8
68. Yetkin-Arik B, Vogels IMC, Nowak-Sliwinska P, Weiss A, Houtkooper RH, Van Noorden CJF, Klaassen I, Schlingemann RO (2019) The role of glycolysis and mitochondrial respiration in the formation and functioning of endothelial tip cells during angiogenesis. Sci Rep. https://doi.org/10.1038/S41598-019-48676-2
69. Yokoyama M, Shimizu I, Nagasawa A, Yoshida Y, Katsuumi G, Wakasugi T, Hayashi Y, Ikegami R, Suda M, Ota Y, Okada S, Fruttiger M, Kobayashi Y, Tsuchida M, Kubota Y, Minamino T (2019) p53 plays a crucial role in endothelial dysfunction associated with hyperglycemia and ischemia. J Mol Cell Cardiol 129:105–117. https://doi.org/10.1016/J.YJMCC.2019.02.010
70. Zaugg M, Lou P-H, Lucchinetti E, Gandhi M, Clanachan AS (2017) Postconditioning with Intralipid emulsion protects against reperfusion injury in post-infarct remodeled rat hearts by activation of ROS-Akt/Erk signaling. Transl Res 186:36-51.e2. https://doi.org/10.1016/j.trsl.2017.05.007
71. Zhang DX, Gutterman DD (2007) Mitochondrial reactive oxygen species-mediated signaling in endothelial cells. Am J Physiol Heart Circ Physiol 292:2023–2031. https://doi.org/10.1152/ajpheart.01283.2006
72. Zudaire E, Gambardella L, Kurcz C, Vermeren S (2011) A computational tool for quantitative analysis of vascular networks. PloS One. https://doi.org/10.1371/journal.pone.0027385